The Effects of Climate Change and Climate Policy on Credit Risk

Matthijs Leegstra[1], Erik Kole*[1,2], and Rasmus Lönn[1,3]

[1] *Econometric Institute, Erasmus School of Economics, Erasmus University Rotterdam*
[2] *Tinbergen Institute*
[3] *Erasmus Research Institute of Management*

February, 2026

Abstract

This study examines how climate-related physical and transition risks affect credit risk. We develop a modular framework based on a threshold model for credit migrations, linking latent credit factors to key economic indicators to measure credit risk in bond markets. Using historical rating migrations, we estimate the model parameters and apply the framework to U.S. data to assess the implications of alternative climate policies. These policies generate projected paths for credit cycles that differ markedly in direction, magnitude, and volatility. These differences translate into substantial variation in both expected losses and tail risks for diversified bond portfolios. Notably, also high-quality bond cohorts are sensitive to policy choices. Comparisons with a continuation of current policies show that orderly transitions, characterized by reduced physical damages and increased transition costs entail higher initial expenses but deliver net savings from 2035 onward. In contrast, disorderly transitions result in steep cost increases after 2030 and overall higher costs by 2050.

Keywords: Corporate credit ratings, climate change, climate-economy models, stress testing, economic capital
JEL classification: E44, G17, G24, Q54

*Authors have made equal contributions. We thank Robin Lumsdaine, Fulvia Marotta, and the audiences of seminars at Cambridge University (climaTRACES), Erasmus University (Econometric Institute), in the conferences "Econometric Models of Climate Change" (University of Victoria, Canada, 2025) and "Social and Sustainable Finance: Bridging Methods, Policy and Practice" (Brunel University, UK, 2025) for useful comments and suggestions. Address: Burg. Oudlaan 50, P.O. Box 1738, 3000DR Rotterdam, The Netherlands, Tel. +31 10 408 12 58. E-mail addresses m.w.leegstra@gmail.com, kole@ese.eur.nl, lonn@ese.eur.nl.

1 Introduction

Risks from climate change can significantly affect financial institutions and financial markets. These risks can be split into physical and transition risks (see e.g., Acharya et al., 2023; BCBS, 2021). Physical risks arise from the adverse effects of greenhouse gas emissions, resulting in heightened vulnerability to physical damages. Transition risks emerge from actions taken to mitigate the impacts of global warming, and can take the form of changes in government policies, technological developments, or shifts in investor and consumer preferences. Both risk types affect the risk profile of firms' cash flows and, hence, the value and riskiness of financial assets. Importantly, they are not independent, but present a trade-off. Maintaining current policies with limited effort to deal with climate change generates small transition risks but considerable physical risks, whereas other transition scenarios may lead to larger transition risks but smaller physical risks, with key differences arising from the timing with which they materialize or recede. Though the financial sector is well aware of these risks (Stroebel and Wurgler, 2021), their incorporation into fundamental risk models still needs attention.[1] This holds in particular for the effects that the evolution of transition risks in different policies has on financial risk.

In this paper, we study how the paths of physical and transition risks stemming from different transition scenarios affect financial risk. We investigate the impact that different scenarios have on the credit risk of corporate bonds with different ratings and on the loss distribution of bond portfolios, taking a systematic risk perspective. Though firms are heterogeneous in their exposure to climate risk such that threats to one firm may be opportunities for another, the systematic part remains present in the financial sector and should be reflected in capital reserves. These capital reserves constitute opportunity costs, which eventually are borne by society. Having better insight into these costs can be beneficial for evaluating the different transition scenarios and comparing, for example, a scenario in which CO_2 emissions reach net-zero in 2050 with one in which countries stick to nationally determined contributions. This systematic risk focus makes our methods generalizable to other assets and other financial risks.

To answer our research question, we propose a modular framework that links transition scenarios via their macroeconomic consequences to credit risk. The first module consists of a factor model for rating migrations of corporate bonds. It takes the form of the CreditMetrics ordered probit model as in Gupton, Finger and Bhatia (1997) and Belkin, Suchower and Forest Jr.

[1] See ECB (2022) and the update in `https://www.bankingsupervision.europa.eu/press/blog/2025/html/ssm.blog20250711~6b58023889.en.html?` for the European, and FED (2024) for the US banking sector.

(1998), which generalizes the default-threshold model of Merton (1974) and Vasicek (2002). The second module is a dynamic linear model that relates the factors from the first module to key economic indicators. The third module combines the previous modules to assess the credit risk of a well-diversified bond portfolio. Extending Vasicek (2002), we derive the asymptotic loss distribution of homogeneous bond portfolios, and show how simulations can generate the loss distribution of heterogeneous portfolios as in Miu and Ozdemir (2006) and Keijsers, Diris and Kole (2018). The economic capital requirement, which act as a buffer against unexpected losses, is then calculated from the loss distribution.

We use this framework to determine the impact that different transition scenarios have on the loss distribution of US corporate bonds. Based on semi-annual rating transitions published by S&P Global over the period 2000 to 2024, we estimate the parameters and the credit cycle of the CreditMetrics module. The second module links the cycle to key economic indicators, such as economic growth, inflation, interest rates, oil prices and equity returns. The third module uses the scenarios produced by the Network of Central Banks and Supervisors for Greening the Financial System (NGFS, 2024b) for the paths of these indicators up to 2050. The scenarios depend on the policies that are adopted as a response to climate change but also on the models for physical and transition risks. In particular, we study six policies that vary in ambition and timeline, combined with three transition models. Two scenarios can be characterized as orderly transitions, where different countries and institutions take rapid and concerted actions to limit climate change. These scenarios combine small physical risks with small to moderate transition risks. The other scenarios are either less ambitious with moderate transition risks but large physical risks, or less timely and orderly with large transition risks as well as moderate to large physical risks. We use the paths of the economic indicators in each scenario to predict the credit cycle and derive the loss distribution of various bond portfolios. This last step produces credit risk dynamics that are consistent with the overall economic developments in each scenario.

Our results show credit cycles within rating cohorts that are strongly related to economic indicators. Differences in exposures to the factors underlying the cycles lead to heterogeneity across the cohorts formed by firms with the same credit rating. The economic paths in the difference scenarios translate into paths for the credit cycle that also vary substantially. The rapid and concerted actions of the orderly transition scenarios lead to a quick drop in the cycle in each cohort. The two scenarios with limited actions lead to a hot-house world in which the credit cycles steady worsen over time. In the remaining two scenarios, transitions are delayed and/or disorderly, and as a consequence the credit cycles remain favorable in the first few years, but exhibit large swings thereafter. A comparison of the credit cycle paths shows that a reduction of physical risks translates into significant improvements, whereas a reduction of transition risks limits cycle volatility.

Changes in the credit cycles affect the loss distribution of bond portfolios and the resulting capital requirements, where we focus on its expectation and 99.9% quantile. The difference between these two gives the economic capital that financial institutions must hold as a buffer against unexpected losses. Though both the expected losses and quantiles are non-linear functions of the credit cycle, their paths in the different scenarios are qualitatively similar to the path of the cycle itself. We assess the change in capital requirements in the different scenarios relative to current policies, both for portfolios with bonds from one rating cohort and for more heterogeneous bond portfolios.

Our empirical results show that transition scenarios have strong implications for credit cycles and the resulting economic capital requirements of bond portfolios. Orderly transition scenarios are associated with pronounced transition related damages in the initial years of the transition, leading to a deterioration of credit conditions and higher economic capital requirements across investment grade cohorts, which at their peak are about 30% higher than in the scenario which merely maintains current policies. These increases occur primarily during the first decade of the transition. As transition related damages dissipate and physical risks remain limited, credit cycles recover and required economic capital declines. From the mid 2030s onward, orderly transition scenarios generally imply lower capital requirements of around 10% than those obtained under a continuation of current policies, resulting in a prolonged period of reduced opportunity costs.

In contrast, delayed and less coordinated transition scenarios maintain more favorable credit conditions in the early years but lead to substantial increases in risk once the transition begins or physical risks materialize. Economic capital becomes more volatile around the transition period in the early 2030s and typically exceeds the levels implied by current policies during this phase. Although capital requirements gradually return to benchmark levels in later years, these scenarios generate extended periods of elevated risk. The relative effects are strongest for investment grade cohorts, whose credit cycles respond more strongly to macroeconomic conditions, while high-yield bonds exhibit smaller proportional changes across scenarios. These qualitative patterns remain present in heterogeneous portfolios that contain a finite number of assets drawn from multiple cohorts, although the magnitude of the effects is smaller due to the presence of idiosyncratic risk. Differences between transition scenarios are therefore less pronounced at the portfolio level, while the timing and ordering of risk across scenarios remain broadly unchanged. Taken together, the results indicate that earlier transition leads to a transitory increase in capital requirements that is offset by reductions in long term physical risk during the 2030s.

Our research contributes to three strands of literature. First, we propose a framework that generates risk measures consistent with the macroeconomic consequences of a specific climate scenario. It extends the climate risk stress test methodology of the European Central Bank that also advocates the use of the NGFS scenarios (see ECB, 2022) by incorporating the impact of transition scenarios on credit cycles through macroeconomic conditions. This integration is one of the challenges for the consequences of climate risk for financial institutions discussed by Baudino and Svoronos (2021). The extension fits well with the Basel IV guidelines prescribed by the Basel Committee on Banking Supervision, in which an asymptotic single risk factor model is used to determine capital requirements for credit risk (see also BCBS, 2005, 2017). It is also in line with the conceptual framework laid out in a survey article by Acharya et al. (2023) about climate stress testing. Their framework consists of three elements: (i) a set of future scenarios of climate change and related policies with their effects on macro indicators, (ii) models that link these indicators to interest rate, market, credit, or other forms of risk and give their effects on (portfolios of) financial assets, and (iii) the consequences for financial institutions in terms of their balance sheets, risk-weighted assets and capital reserves. Reinders, Schoenmaker and van Dijk (2025) propose a similar framework with the additional step of a "satellite model" that links the macro indicators to financial indicators (see also Roger and Vlcek, 2012). Similarly, our framework shows how climate risk can be incorporated into the general macro stress test discussed in Borio, Drehmann and Tsatsaronis (2014). It complements studies that look at actual bank exposures like Jung, Santos and Seltzer (2023) or stress tests with more specific scenarios like Reinders, Schoenmaker and van Dijk (2023).

Second, we contribute to the literature on credit risk modeling. We extend the static framework of Gupton et al. (1997), Belkin et al. (1998), and Vasicek (1991) by allowing the credit cycles to depend on contemporaneous economic indicators. Because the commonality in credit migrations is not necessarily fully driven by these economic indicators, our approach accommodates the presence of a frailty factor that has been widely documented for defaults, see e.g., McNeil and Wendin (2007), Koopman and Lucas (2008), Duffie, Eckner, Horel and Saita (2009), Koopman, Lucas and Schwaab (2012), and Schwaab, Koopman and Lucas (2016), and for credit migrations by Koopman, Lucas and Monteiro (2008). We deviate from the mixed-measurement models proposed by Creal, Schwaab, Koopman and Lucas (2014), Schwaab et al. (2016), and Keijsers et al. (2018), where probabilities of default and macro variables are all adapted to the same latent processes. Because of the direct link between the economic indicators and the credit cycles, we can plug in the NGFS scenarios and directly determine the consequences for the cycles.

Third, our research contributes to the larger field of climate finance by showing how different paths for physical and transition risks affect the risk profile of corporate bonds with different ratings. This result complements research into the valuation of fixed income instruments such as Painter (2020), Javadi and Masum (2021), and Acharya, Johnson, Sundaresan and Tomunen (2022), showing that physical risk is priced, and Seltzer, Starks and Zhu (2022) showing the pricing of transition risk. Our focus on corporate bonds complements Klusak, Agarwala, Burke, Kraemer and Mohaddes (2023), who show that climate change can lead to a substantial deterioration in sovereign credit ratings based on projections up to 2100. The different effects of physical and transition risks may require separate treatment in more structural models capturing the interplay between economic processes of consumption and production, asset prices and climate, such as Bansal, Kiku and Ochoa (2019), Giglio, Kelly and Stroebel (2021), Giglio, Maggiori, Rao, Stroebel and Weber (2021), and Cosemans, Hut and Van Dijk (2021).

From a practical perspective, our proposed framework and results contribute to the discussion on how to deal with climate change from a financial risk standpoint. Orderly transitions with coordinated and timely actions can reduce physical risks with limited increases in transition risks. They initially bring larger costs but lead to net savings over the full period to 2050. Disorderly transitions lead to a smaller reduction in physical risk and substantial transition risk, which produces a volatile and negative path for the credit factor. Although having lower costs at first, the net effect shows that delaying actions imposes larger costs on the financial sector and hence on society.

Our paper is organized as follows. Section 2 presents our econometric framework and estimation. Section 3 presents the migration data, key economic indicators, and the NGFS scenarios. We present the in-sample results in Section 4 and turn to the out-of-sample results in Section 5. Section 6 presents the conclusion and discussion. We present additional results in an appendix.

2 Methodology

In this section, we present the model that we use to investigate how the transition scenario impacts credit risk and the resulting economic costs for diversified bond portfolios of different credit quality. The central concept in our framework is a set of latent factors $\boldsymbol{F}_t$ that capture the credit cycle. All bonds are exposed to the credit cycle, so for each bond, the probability of a credit migration, of which default is one outcome, depends on $\boldsymbol{F}_t$. The actual exposures of a bond to the latent factors depend on its current credit rating, which we use to define cohorts. We relate the credit cycle to a set of key economic indicators. By combining these two parts, we can determine the impact of a transition scenario on the credit cycle and, consequently, on the bonds in a particular cohort. We make this impact concrete by comparing the expected losses and economic capital required for bond cohorts and for diversified bond portfolios under different transition scenarios.

2.1 The latent factor model for credit risk

The starting point of our methodology is the ordered probit model of CreditMetrics for credit rating transitions as proposed in Belkin et al. (1998). This model generalizes the threshold view of default in Merton (1974) and Vasicek (2002), which states that default occurs when a firm's equity is depleted or, in other words, when the value of its assets falls below its liabilities.[2] The CreditMetrics model incorporates all types of credit migration, recognizing that default is just one specific outcome within the broader context of credit migration. In this model, the credit rating S_{it} of the firm i at time t is a categorical variable that reflects the probability that the firm will default through the cycle. We assume that there are q rating categories $j = 1, \ldots, q$, with 1 being the highest rating and q being the lowest, which indicates that the firm is already in default at time t. The final state $S_{it} = q$ is an absorbing state, so firms in default will remain so.

Because a firm's financial conditions change over time, the credit rating of a firm's bonds can change. We assume that the rating follows a first-order Markov chain, that is, the rating distribution at time t depends only on the rating at $t-1$, $\Pr[S_{it} = j|S_{i,t-1}, S_{i,t-2}, \ldots] = \Pr[S_{it} = j|S_{i,t-1}]$. As in Belkin et al. (1998), this conditional probability reflects a latent variable Y_{it} that can be interpreted as a credit change indicator, with a low value indicating a worsening of a

[2]This model abstracts from the actual event that triggers a default, i.e. arrears in payments or filing for bankruptcy protection.

firm's credit position.

Next, we define sets of $q-1$ ordered thresholds $K_{1m} > K_{2m} > \ldots > K_{q-1,m}$ for $m = 1, \ldots, q-1$ to give the probability $p_{jm} = \Pr[S_{it} = j | S_{i,t-1} = m]$ of a transition from state $m = 1, \ldots, q-1$ to j as

$$p_{jm} = \begin{cases} \Pr[Y_{it} > K_{1m} | S_{i,t-1} = m] & \text{for } j = 1, \\ \Pr[K_{jm} < Y_{it} \leq K_{j-1,m} | S_{i,t-1} = m] & \text{for } j = 2, \ldots, q-1, \\ \Pr[Y_{it} \leq K_{q-1,m} | S_{i,t-1} = m] & \text{for } j = q. \end{cases} \tag{1}$$

Since the default state q is absorbing, we have $p_{qq} = 1$ and $p_{jq} = 0$ for $j \neq q$.

To capture the presence of a credit cycle in which periods of many downgrades and few upgrades alternate with periods of few downgrades and many upgrades, we follow Gordy and Heitfield (2010); Pfeuffer, Nagl, Fischer and Rösch (2020) and assume that each firm is exposed to r common factors $\boldsymbol{F}_t$,

$$Y_{it} = \boldsymbol{\lambda}_i' \boldsymbol{F}_t + \sigma_i \varepsilon_{it}, \tag{2}$$

where $\boldsymbol{\lambda}_i$ denotes the r-vector of factor loadings and ε_{it} is an idiosyncratic component. The idiosyncratic components for different firms are assumed to be independent. This formulation can be seen as a structural model for the credit change indicator, or as a factor model such as those that are widely used in finance and macroeconomics (see e.g. Cochrane, 2005; Stock and Watson, 2016). An important difference is that Y_{it} is latent, and hence identifying restrictions are needed. It is common in this literature to impose that all random variables Y_{it}, $\boldsymbol{F}_t$, and ε_{it} follow standard normal distributions. As a consequence, $-1 < \lambda_{ij} < 1$ for $j = 1, \ldots, r$, $\boldsymbol{\lambda}_i' \boldsymbol{\lambda}_i < 1$ and $\sigma_i = \sqrt{1 - \boldsymbol{\lambda}_i' \boldsymbol{\lambda}_i}$. Since Y_{it} follows a normal distribution, the model for credit migrations in eq. (1) becomes an ordered probit model.

In addition to these identification restrictions, the literature typically assumes that firms in the same cohort, defined by one or more characteristics, have the same exposure to the common factor. We group firms by initial credit rating $S_{i,t-1} = m$, so $\boldsymbol{\lambda}_i = \boldsymbol{\lambda}_j$ if $S_{i,t-1} = S_{j,t-1}$ and we consequently write $\boldsymbol{\lambda}_m$. Consequently, the model in eq. (2) can be rewritten as

$$Y_{it} = \boldsymbol{\lambda}_m' \boldsymbol{F}_t + \sqrt{1 - \boldsymbol{\lambda}_m' \boldsymbol{\lambda}_m} \varepsilon_{it}. \tag{3}$$

The correlation ρ_m between two firms i and j in the same cohort equals $\mathrm{E}[Y_{it} Y_{jt}] = \boldsymbol{\lambda}_m' \boldsymbol{\lambda}_m$. The correlation between two firms i and j in different cohorts is equal to $\boldsymbol{\lambda}_i'\boldsymbol{\lambda}_j$, which is referred to as inter-cohort correlation (see Pfeuffer et al., 2020).

Latent factor models generally exhibit the property that the factors and loadings are not uniquely defined (see Stock and Watson, 2016). In this case, the factors and loadings in eq. (3) can be replaced by $\boldsymbol{Q}\boldsymbol{F}_t$ and $\boldsymbol{\lambda}_m\boldsymbol{Q}'$ where $\boldsymbol{Q}$ is an orthogonal matrix. Because the product of factors and loadings is unique per cohort, it is convenient to write eq. (3) as a single factor model,

$$Y_{it} = \sqrt{\rho_m} Z_{mt} + \sqrt{1-\rho_m}\varepsilon_{it}, \tag{4}$$

where $Z_{mt} = \boldsymbol{\lambda}_m'\boldsymbol{F}_t / \sqrt{\boldsymbol{\lambda}_m'\boldsymbol{\lambda}_m}$, where the scaling ensures Z_{mt} has a standard normal distribution. As such, for each cohort, Z_{mt} is a unique factor that drives the cyclical variation in migrations.

We model each factor Z_{mt} using a simple dynamic linear model with a set of k business cycle indicators $\boldsymbol{X}_t$ and the lagged realization of Z_{mt}

$$Z_{mt} = \boldsymbol{\beta}_m'\boldsymbol{X}_t + \phi_m Z_{m,t-1} + \psi_m \eta_{mt}, \quad \eta_{mt} \sim \mathrm{N}(0,1), \tag{5}$$

where $\boldsymbol{\beta}_m$ is a k-vector of coefficients, ϕ_m and ψ_m are scalar coefficients and η_{mt} is an innovation independent of $\boldsymbol{X}_t$, $Z_{m,t-1}$, and ε_{it} for all i. Because η_{mt} is common to all bonds in cohort m, and independent of the business cycle indicators, it can be interpreted as a frailty factor as in Duffie et al. (2009); Koopman and Lucas (2008); Koopman et al. (2012); Schwaab et al. (2016). Because Z_{mt} has unit variance by construction, the residual variance is restricted to $\psi_m^2 = 1 - \phi_m^2 - \boldsymbol{\beta}_m'\boldsymbol{\Sigma}_{\boldsymbol{X}}\boldsymbol{\beta}_m$, where $\boldsymbol{\Sigma}_{\boldsymbol{X}}$ is the covariance matrix of the business cycle indicators, and as a result, $0 \leq \phi_m^2 + \boldsymbol{\beta}_m'\boldsymbol{\Sigma}_{\boldsymbol{X}}\boldsymbol{\beta}_m \leq 1$. This specification with a cohort-specific factor Z_{mt} as dependent variable corresponds to a linear model for $\boldsymbol{F}_t$, but is easier to interpret as Z_{mt} is uniquely identified.

2.2 Implications for risk management

The credit risk of a portfolio of bonds can be analyzed in the point-in-time (PIT) or the through-the-cycle (TTC) setting.[3] In the PIT setting, the common factors are treated as given or predicted, whereas in the TTC setting, they are averaged out (see e.g. Carlehed and Petrov,

[3]Accounting regulations in IFRS9 prescribe the use of a forward-looking PIT probability of default to determine expected losses, see `https://www.ifrs.org/issued-standards/list-of-standards/ifrs-9-financial-instruments.html/`. The Basel Framework prescribes the use of 1-year TTC probabilities of default to calculate unexpected losses to determine required capital reserves, see `https://www.bis.org/baselframework/BaselFramework.pdf`.

2012; Yang, 2014). We will use the NGFS scenarios to create paths of the predicted probability of default at each point in time, which we will then use to derive risk measures for portfolios of bonds. This approach can be seen as a hybrid, as we use the effect of the NGFS scenarios as given, but we do not make further assumptions about the state of the credit cycle. We consider two types of portfolio, one with infinitely many bonds of the same cohort, in which case we derive closed-form expressions for the risk measures, and one with a fixed number of bonds of different cohorts, in which case we revert to simulations.

With information about the common factors, the probability that a bond migrates from rating cohort m to j at time t becomes $p_{jm}(\mathcal{I}_t) = \Pr[S_{i,t} = j | S_{i,t-1} = m, \mathcal{I}_t]$. $\mathcal{I}_t$ is the information set that contains Z_{mt} or $(\boldsymbol{X}_t, Z_{m,t-1})$. This probability is derived from eq. (1)

$$p_{jm}(\mathcal{I}_t) = \begin{cases} 1 - \Phi((K_{j,m} - \mu_{mt})/\sigma_m) & \text{for } j = 1, \\ \Phi((K_{j-1,m} - \mu_{mt})/\sigma_m) - \Phi((K_{j,m} - \mu_{mt})/\sigma_m) & \text{for } j = 2, \ldots, q-1, \\ \Phi((K_{j-1,m} - \mu_{mt})/\sigma_m) & \text{for } j = q, \end{cases} \tag{6}$$

where we use the fact that the distribution of Y_{it} conditional on $S_{i,t-1}$ and $\mathcal{I}_t$ follows a normal distribution $\mathrm{N}(\mu_{mt}, \sigma_m^2)$ with $\Phi(\cdot)$ denoting its standard cdf. The parameters μ_{mt} and σ_m^2 depend on the information set

$$\big(\mu_{mt}, \sigma_m^2\big) = \begin{cases} \big(\sqrt{\rho_m} Z_{mt}, 1 - \rho_m\big) & \text{if } \mathcal{I}_t = Z_{mt} \\ \big(\sqrt{\rho_m}(\boldsymbol{\beta}_m' \boldsymbol{X}_t + \phi_m Z_{m,t-1}), 1 - \rho_m(1 - \psi_m^2)\big) & \text{if } \mathcal{I}_t = \{\boldsymbol{X}_t, Z_{m,t-1}\}. \end{cases} \tag{7}$$

The variance in the second case follows as $\mathrm{Var}[Y_{it} | S_{i,t-1} = m, \boldsymbol{X}_t, Z_{m,t-1}] = \mathrm{Var}[\sqrt{\rho_m}\eta_{mt} + \sqrt{1-\rho_m} \cdot \varepsilon_{it} | \boldsymbol{X}_t, Z_{m,t-1}] = \rho_m \psi_m^2 + 1 - \rho_m = 1 - \rho_m(1 - \psi_m^2)$. Since $0 \leq \psi_m^2 \leq 1$, the variance of the second case exceeds that of the first case and the difference reflects the additional uncertainty due to predicting Z_{mt} rather than conditioning on it.

Our focus is on the risk of a bond portfolio. We assume that at the start of period t the portfolio consists of N_{mt} bonds with rating m, which we gather in the vector $\boldsymbol{N}_t$ of size $q-1$. For each bond with rating m, γ_{im} denotes the exposure at default and λ_{im} the loss given default as a proportion of the exposure at default, which we assume to be deterministic or independent of the common factor, from each other and from other bonds.[4] The loss at the end of period t,

[4]Evidence in Frye (2000); Keijsers et al. (2018); Schuermann (2004) shows larger LGDs during economic downturns, but given the paucity of data, we leave inclusion of this dependence for future research.

$L_t(\boldsymbol{N}_t)$, is a random variable given by

$$L_t(\boldsymbol{N}_t) = \sum_{m=1}^{q-1} \sum_{i=1}^{N_{mt}} \gamma_{im} \lambda_{im} I(Y_{imt} \leq K_{q-1,m}), \tag{8}$$

where $I(\bullet)$ denotes the indicator function.

The expected loss of this portfolio conditional on the information set $\mathcal{I}_t$ follows directly as

$$\mathrm{E}[L_t(\boldsymbol{N}_t)|\mathcal{I}_t] = \sum_{m=1}^{q-1} \sum_{i=1}^{N_{mt}} \gamma_{im} \lambda_{im} p_{qm}(\mathcal{I}_t), \tag{9}$$

where the probability of default $p_{qm}(\mathcal{I}_t)$ is given in eq. (6). To determine the economic capital, which is defined as the difference between the Value-at-Risk with confidence level α and the expected loss of the portfolio, the α-quantile of $L_t(\boldsymbol{N}_t)$ is required. In the asymptotic setting of Vasicek (1991, 2002), this quantile can be derived in closed form, and otherwise simulations can be used. We will discuss both.

In the setting of Vasicek (1991, 2002), it is assumed that $\gamma_{im} = \lambda_{im} = 1$. Under these assumptions, the percentage loss of a bond portfolio consisting solely of bonds with rating m is calculated as

$$\delta(N_{mt}) = L_t(N_{mt})/N_{mt} = \sum_{i=1}^{N_{mt}} I(Y_{imt} \leq K_{q-1,m})/N_{mt}. \tag{10}$$

We show in appendix A that the distribution of the percentage loss $\delta_{mt} = \lim_{N_{mt}\to\infty} \delta(N_{mt})$ follows

$$\Pr[\delta_{mt} \leq v|\boldsymbol{X}_t, Z_{m,t-1}] = \Phi\left(\frac{\sqrt{1-\rho_m}\Phi^{-1}(v) + \mu_{mt} - K_{q-1,m}}{\sqrt{\rho_m}\psi_m}\right). \tag{11}$$

This result extends Vasicek (1991) to the case where the common factor is predicted. The α-quantile of the distribution of δ_{mt} is obtained by inverting $\Pr[\delta_{mt} \leq v|\mathcal{I}_t] = \alpha$,

$$v_{mt}(\alpha; \boldsymbol{X}_t, Z_{m,t-1}) = \Phi\left(\frac{\sqrt{\rho_m}\psi_m\Phi^{-1}(\alpha) - \mu_{mt} + K_{q-1,m}}{\sqrt{1-\rho_m}}\right). \tag{12}$$

Hence the economic capital at confidence level α for this asymptotic portfolio at time t equals

$$EC_\alpha^{\mathrm{as}}(m; \boldsymbol{X}_t, Z_{m,t-1}) = v_{mt}(\alpha; \boldsymbol{X}_t, Z_{m,t-1}) - p_{qm}(\boldsymbol{X}_t, Z_{m,t-1}). \tag{13}$$

This expression for economic capital corresponds to a limiting portfolio consisting solely of bonds of one rating category. The result can hence be interpreted as an upper bound on the effect of a particular scenario at time t on a portfolio of bonds with credit rating m. In this portfolio, all idiosyncratic effects have been diversified, so the portfolio risk is completely driven by the systematic component. Using this risk measure to compare rating categories can then show which cohorts are most sensitive to climate risk.

If not all idiosyncratic risk has been diversified or assets are heterogeneous in credit quality, the closed-form expressions above can be replaced by simulations to evaluate the loss distribution in eq. (8). For a given information set, simulate a realization for the credit indicator for each bond in the portfolio as $\tilde{Y}_{imt} = \mu_{mt} + \tilde{e}_{imt}$, where

$$\tilde{e}_{imt} = \begin{cases} \sqrt{1-\rho_m}\tilde{\varepsilon}_{imt} & \text{if } \mathcal{I}_t = Z_{mt} \\ \psi_m \boldsymbol{\lambda}_m' \tilde{\boldsymbol{u}}_t + \sqrt{1-\rho_m}\tilde{\varepsilon}_{imt} & \text{if } \mathcal{I}_t = \{\boldsymbol{X}_t, Z_{mt-1}\}, \end{cases} \tag{14}$$

where the elements of $\tilde{\varepsilon}_{imt}$ and $\tilde{\boldsymbol{u}}_t$ are uncorrelated and follow standard normal distributions. In the second case of (2.2), defaults are correlated, which is accounted for by the draw $\tilde{\boldsymbol{u}}_t$ which is common to all bonds in all cohorts. The simulated loss is given by $\tilde{L}_t(\boldsymbol{N}_t) = \sum_{m=1}^{q-1}\sum_{i=1}^{N_{mt}} \gamma_{im}\lambda_{im} I(\tilde{Y}_{imt} \leq K_{q-1,m})$. Repeating this procedure many times gives the distribution of $L_t(\boldsymbol{N}_t)$ from which the α-quantile can then be calculated.

2.3 Estimation

The estimation procedure consists of four steps. First, we use a sample of credit transitions observed over T periods to consecutively estimate the thresholds K_{jm}, the factor loadings $\boldsymbol{\lambda}_m$, and factor realizations $\boldsymbol{F}_t$. We then use these realizations to construct the implied Z_{mt} series and estimate the parameters $\boldsymbol{\beta}_m$ and ϕ_m in the dynamic linear model in eq. (5) for each cohort.

Let D_{jmt} denote the number of bonds migrating from rating m to j during period t. Because the default state q is absorbing, m runs from 1 to $q-1$. $\boldsymbol{D}_t$ denotes the set of all migrations during period t. Conditional on $\boldsymbol{F}_t$, the set of migrations $\{D_{jmt}\}_{j=1}^{q}$ from a given cohort m follows a multinomial distribution, parametrised by the q transition probabilities $p_{jm}(Z_{mt})$. They are a function of the thresholds K_{jm} in eq. (6) and the factor loadings $\boldsymbol{\lambda}_m$ in eq. (3). The probability mass function for $\boldsymbol{D}_t$ follows as

$$\Pr[\boldsymbol{D}_t|\boldsymbol{F}_t;\boldsymbol{\Lambda},\boldsymbol{K}] = \prod_{m=1}^{q-1} N_{mt}! \prod_{j=1}^{q} \frac{(p_{jm}(\boldsymbol{F}_t))^{D_{jmt}}}{D_{jmt}!}, \tag{15}$$

where $N_{mt} = \sum_{j=1}^{q} D_{jmt}$ gives the number of firms in cohort m at the start of t, $\boldsymbol{\Lambda}$ is the $q-1 \times r$

matrix with factor loadings, and $\boldsymbol{K}$ the $q-1 \times q-1$ matrix with thresholds K_{jm}. It is the product of $q-1$ multinomial pmfs because conditional on $\boldsymbol{F}_t$, transitions from different cohorts are independent. The unconditional probability at t follows as

$$\Pr[\boldsymbol{D}_t; \boldsymbol{\Lambda}, \boldsymbol{K}] = \int_{\mathbb{R}^r} \Pr[\boldsymbol{D}_t | \boldsymbol{F}_t; \boldsymbol{\Lambda}, \boldsymbol{K}] \, \mathrm{d}\Phi_r(\boldsymbol{F}_t), , \tag{16}$$

where $\boldsymbol{\Phi}_r$ denotes the r-variate standard normal density.

We estimate $\boldsymbol{K}$ using a method of moments estimator as in Gordy and Heitfield (2010) and Belkin et al. (1998). This estimator uses the result that the unconditional distribution of each firm's credit change indicator Y_{it} in a particular cohort m follows a standard normal distribution as given by eq. (3). Combining this result with eq. (1) implies that the unconditional transition probabilities p_{jm} satisfy

$$p_{jm} = \begin{cases} 1 - \Phi(K_{1m}) & \text{for } j = 1, \\ \Phi(K_{jm}) - \Phi(K_{j-1,m}) & \text{for } j = 2, \ldots, q-1, \\ \Phi(K_{qm}) & \text{for } j = q. \end{cases}$$

Estimating the unconditional probabilities by the average rates $\bar{p}_{jm} = \frac{1}{T} \sum_{t=1}^{T} D_{jmt}/N_{mt}$ and inverting the above equation leads to the estimator

$$\hat{K}_{jm} = \Phi^{-1} \left(1 - \sum_{k=1}^{j} \bar{p}_{km} \right) \quad \text{for } j = 2, \ldots, q-1. \tag{17}$$

Gordy and Heitfield (2010) show that this estimator has negligible bias, also for small realistic sample sizes.

To calculate the likelihood, we need to integrate over the latent factor realizations $\boldsymbol{F}_t$, which follow a standard normal distribution. We approximate this integral by taking S draws $\boldsymbol{F}_s$ of a vector of independent standard normal random variables, yielding an approximate likelihood for period t,

$$\mathcal{L}_t(\boldsymbol{D}_t, \boldsymbol{N}_t; \boldsymbol{\Lambda}, \boldsymbol{K}) = \frac{1}{S} \sum_{s=1}^{S} \Pr[\boldsymbol{D}_t | \boldsymbol{F}_s; \boldsymbol{\Lambda}, \boldsymbol{K}). \tag{18}$$

The log likelihood to optimize then follows as

$$\ell(\boldsymbol{\Lambda}, \boldsymbol{K}) = \sum_{t=1}^{T} \log \mathcal{L}_t(\boldsymbol{D}_t; \boldsymbol{\Lambda}, \boldsymbol{K}) = C + \sum_{t=1}^{T} \log \sum_{s=1}^{S} \prod_{m=1}^{q-1} \prod_{j=1}^{q} p_{jm}(\boldsymbol{F}_s)^{D_{jmt}}, \tag{19}$$

where we suppress the dependence of ℓ on the series $\boldsymbol{D}_t$ to ease the notation, and C collects the constant terms. The estimator $\hat{\boldsymbol{\Lambda}}$ maximizes this expression,

$$\hat{\boldsymbol{\Lambda}} = \arg \max_{\boldsymbol{\lambda}_m : \boldsymbol{\lambda}_m' \boldsymbol{\lambda}_m < 1} \ell(\boldsymbol{\Lambda}, \hat{\boldsymbol{K}}), \tag{20}$$

with $\hat{\boldsymbol{K}}$ as in eq. (17). Because the loadings are identified up to a rotation by an orthogonal matrix, we impose that all $q-1$ cohorts load on the first factor, only $q-2$ cohorts load on the second factor, and so on. [5]

For given values of $\boldsymbol{\Lambda}$ and $\boldsymbol{K}$, one way to determine $\hat{\boldsymbol{F}}_t$ is to maximize the log likelihood at each point in time t as a function of $\boldsymbol{F}_t$, i.e.

$$\hat{\boldsymbol{F}}_t = \arg \max_{\boldsymbol{F}_t} \sum_{m=1}^{q-1} \sum_{j=1}^{q} D_{jmt} \log p_{jm}(\boldsymbol{F}_t). \tag{21}$$

This maximization differs from the one in Belkin et al. (1998), who propose to estimate the factor realization as the solution to a weighted least-squares problem. Their approach is less appealing because it ignores the multinomial distribution of credit migrations.

In the final step, we construct the cohort-specific factor realizations $\hat{Z}_{mt} = \hat{\boldsymbol{\lambda}}_m' \hat{\boldsymbol{F}}_t$ and use a linear regression to estimate the parameters $\boldsymbol{\beta}_m$ and ϕ_m in eq. (5), treating the realizations as observed. To impose the restriction $\mathrm{E}[Z_{mt}] = 0$, we demean all variables in $\boldsymbol{X}_t$ as is common in the factor model literature (see e.g., Stock and Watson, 2016).

3 Data

3.1 Credit migrations

We use historical semi-annual corporate transition matrices from Standard & Poor's Credit Market Services Limited (S&P) to estimate latent factors. We restrict our attention to firms in the United States that are classified as corporate institutions, excluding financial and insurance institutions. The dataset covers transitions from January 2000 to June 2024 and is publicly available on the website of the European Securities and Markets Authority (ESMA).[6],[7]

[5]The probability $\Pr[D_{1mt}, \ldots, D_{qmt} | \boldsymbol{F}_s] = N_{mt}! \prod_{j=1}^{q} \frac{(p_{jm}(\boldsymbol{F}_s))^{D_{jmt}}}{D_{jmt}!}$ can fall below numerical precision for certain values of Z_s, in which case we remove that particular draw. For our sample, this happens in less than 1% of the draws.

[6]ESMA (2024): "Central Repository of Ratings (CEREP) for publishing the rating activity statistics and rating performance statistics of credit rating agencies". `https://registers.esma.europa.eu/cerep-publication/`

[7]We label the data matrices by the mid-points of the 6-month period, *i.e.*, April 1 and October 1.

S&P distinguishes nine performing rating cohorts (AAA to C), three default cohorts (Default, Selective Default, Regulatory Supervision), and the categories "Non-rated" and "Withdrawals". We exclude bonds in these last two categories from our analysis. Next, we merge the three default cohorts and some of the performing cohorts to ensure a sufficient number of assets and transitions between the different cohorts. We merge the performing cohorts that have the same risk weight according to the EU's Capital Requirements Regulation (see appendix B for more information), that is AAA and AA, as well as B, CCC, CC, and C (denoted as AAA–AA and B–C). As shown in table 1, the AAA–AA cohort is the smallest with an average number of 47 bonds, whereas the B–C cohort is the largest (868 bonds). The cohort sizes show substantial variation over time. In each cohort, the number of bonds tend to increase over time.

Table 1: Cohort sizes and credit migrations

Initial Cohort	Min.	Av.	Max.	End-of-period cohort AAA–AA	A	BBB	BB	B–C	Default
AAA–AA	29	47	131	95.39	4.13	0.46	0.008†	0.008†	0.008†
A	222	280	367	0.25	96.26	3.39	0.045	0.029	0.022
BBB	454	520	615	0.032	1.23	96.64	1.83	0.219	0.047
BB	331	427	500	0.010	0.028	1.84	93.28	4.73	0.11
B–C	513	868	1191	0.001†	0.036	0.036	1.99	96.46	1.47

This table presents the size of each cohort at the start of the period (minimum, average, and maximum number of bonds), and the average relative frequency (in %) of migrations. Migrations are measured semi-annually during the period January 2000 to June 2024 ($T = 49$). AAA–AA and B–C denote the merged cohorts of AAA and AA, and B, CCC, CC and C. A † indicates that no migration has been observed over the sample period. In these cases, we assign a hypothetical half transition (1/2) to the period with the largest cohort size for the computations.

The unconditional migration probabilities in table 1 highlight that transitions within six-month periods are generally rare. The relative frequency of assets migrating to a lower rating is below 5 percent, and less than 2 percent of assets enter default. The cohort subject to the most transitions is the BB cohort, in which around 6.7 percent of assets tend to migrate. The low frequency of transitions emphasizes the importance of maintaining a large cross-section of assets to obtain accurate estimates of the underlying factor structure.

3.2 Economic indicators

The economic indicators consist of macroeconomic variables retrieved from the FRED Database of the Federal Reserve Bank of St. Louis and equity market returns taken from Kenneth French's data library.[8] The macroeconomic variables consist of the growth rate of GDP, the inflation rate,

[8] Available at `https://fred.stlouisfed.org/` and `https://mba.tuck.dartmouth.edu/pages/faculty/ken.french/data_library.html`.

the change in the crude oil prices, and the 10-year real interest rate. Equity market returns are measured based on the value-weighted portfolio of all common stocks on the NYSE, AMEX, and NASDAQ. These data account for various effects arising from macroeconomic, monetary and financial shocks.

The nature of corporate debt data introduces a subtle timing puzzle with respect to economic indicators. We do not observe the exact timing of credit migration between cohorts; rather, we observe end-of-period summaries of the transitions that occurred. We generally expect economic indicators to lead. For example, low GDP growth reduces firms' expected future cash flows, which may trigger a credit downgrade. Though the bankruptcy of a large firm or downgrades of a few large firms may have economy-wide consequences, we do not account for this possibility. As such, we lag the economic indicators by a quarter, meaning that we relate the credit cycle factor corresponding to the first half of year t with the economic indicators observed over the last quarter of year $t-1$ and the first quarter of year t. We present summary statistics and graphs of the time series in Appendix B.2.

3.3 Climate policies and economic scenarios

The Network of Central Banks and Supervisors for Greening the Financial System (NGFS) constructs scenarios "to provide a common starting point for analysing the impact of climate risks on the economy and financial system" (NGFS, 2024b). The scenarios reflect different paths that depend on the evolution of climate change, transition policies, technological and macro-financial developments, and are internally consistent. We use their scenarios, released as NGFS Phase V in November 2024, as predictions for the economic indicators presented in the previous section.[9]

The NGFS distinguishes six different sets of policy ambition, measures and timing, and consequent technological changes. We present their names, descriptions, and risk characterization in table 2. The *Net Zero 2050* and *Below* $2\,^{\circ}C$ scenarios can be seen as *orderly* transitions with low physical risk and limited transition risk. The *Delayed Transition* scenario is *disorderly* with a high degree of transition risks and an intermediate degree of physical risks. The scenarios *Current Policies* and *NDCs* are characterized as *hot house world* with high physical but low transition risks. The *Fragmented World* scenario is *too little, too late* with high risks in both dimensions.

[9] The scenarios are available at www.ngfs.net.

Table 2: Overview of transition scenarios and their descriptions.

Scenario Name	**Description**	**Risk characterization**		
		P	T	Type
Below 2 °C	Increasingly strict policies give approximately a 67% chance of keeping warming below 2 °C, and countries with net-zero targets achieve 80% of their goals.	-	+/-	Orderly
Net Zero 2050	Forceful action and innovation will limit global warming to 1.5 °C, with net-zero CO_2 emissions reached around 2050.	--	+	Orderly
Delayed Transition	Policy action is postponed until 2030, after which decisive measures limit warming to below 2°C.	-	++	Disorderly
Fragmented World	Current policies are maintained until 2030, after which countries with net-zero targets partially meet them by 2050, while countries without such targets continue current policies with no further action.	+	++	Too little, too late
Current Policies	Only currently implemented policies are preserved.	++	--	Hot house world
NDCs	Nationally Determined Contributions; beyond current policies, all pledged targets are met.	+	-	Hot house world

This table reports for each transition scenario its name, description, and a risk characterization with regard to its physical risk (P) and transition risk (T), and the resulting combination (under "Type"). The risk categorization labels are very high (++), high (+), intermediate (+/−), low (-) and very low(--). The information in this table has been taken from NGFS (2024b, p. 8–9).

To determine the impact of these different scenarios, the NGFS combines models for acute and chronic physical risks with models for transition risks. These latter take the form of so-called Integrated Assessment Models (IAMs) that determine the impact on a wide array of economic activities, land uses, and emissions. The NGFS considers three different IAMs, namely REMIND-MAgPIE (REMIND), Global Change Analysis Model (GCAM) and MESSAGEix-GLOBIOM (MESSAGEix), to which we refer by their short name in parentheses. These models share a common goal of modeling the interaction between the economy and the environment, in particular the energy system and land use, but differ with respect to assumptions, granularity, equilibrium type and solution method, see NGFS (2024a). The macro-financial consequences of physical and transition risks are taken from the National Institute Global Econometric Model (NiGEM).[10] We use the predictions from all three IAMs.

The predictions provided in NiGEM correspond to annual effects on economic variables in the different scenarios. We add these effects to the baseline predictions of these variables, also

[10] Created by the National Institute of Economic and Social Research, `https://niesr.ac.uk/`. The NiGEM reports damages to the respective economic indicators relative to a benchmark scenario. We transform all these damages to growth rates that match those obtained from the historical data.

produced by NiGEM. To align these out-of-sample data with the semi-annual estimates from the in-sample period, we interpolate the annual series using cubic splines. From the levels of the economic variables, we compute the changes to obtain series that are analogous to those used in the in-sample data.

Table 3 shows the means of the economic indicators resulting from the different scenarios and IAMs. The means in the baseline scenarios show no or only small differences between the IAMs, meaning that differences between the other scenarios reflect differences in the impact of climate change and policies in the IAMs. The means are also in line with the historical averages over the 2000–2024 period reported in table 8. In all policies and IAMs, incorporating climate change leads to small decreases in the average economic growth and equity market return, and small increases in inflation and the long-term real interest rate. The response of the oil price varies widely over the scenarios and IAMs.

Table 3: Mean of the economic indicators in the NGFS scenarios

		g	π	p	i	e
GCAM	Baseline	3.12	4.25	0.50	1.22	6.68
	Below 2°C	2.56	4.63	11.41	1.69	5.54
	Current Policies	2.40	4.61	0.50	1.22	6.01
	Delayed transition	2.41	4.78	17.06	1.57	6.30
	Fragmented World	2.34	4.77	10.00	1.46	6.11
	Nationally Determined Contributions (NDCs)	2.36	4.70	5.27	1.41	6.02
	Net Zero 2050	2.61	4.65	19.98	1.86	5.54
MESSAGEix	Baseline	3.39	4.25	0.50	1.22	6.68
	Below 2°C	2.80	4.62	2.91	1.50	5.84
	Current Policies	2.67	4.61	0.50	1.22	5.92
	Delayed transition	2.68	4.74	2.95	1.47	6.24
	Fragmented World	2.70	4.64	−3.20	1.30	5.98
	Nationally Determined Contributions (NDCs)	2.70	4.68	0.28	1.42	6.22
	Net Zero 2050	2.84	4.64	11.54	1.95	5.27
REMIND	Baseline	3.15	4.25	0.50	1.22	6.68
	Below 2°C	2.55	4.59	4.98	1.41	6.18
	Current Policies	2.30	4.66	0.50	1.22	5.86
	Delayed transition	2.39	4.76	15.71	1.53	6.59
	Fragmented World	2.35	4.70	5.98	1.31	6.21
	Nationally Determined Contributions (NDCs)	2.36	4.72	8.03	1.53	6.38
	Net Zero 2050	2.79	4.41	15.68	1.70	5.89

This table reports the means of the economic indicators collected from the NGFS data library for the seven scenarios and three Integrated Assessment Models. Variables are annualized and expressed in percent. We denote GDP growth by g, inflation by π, oil price changes by p, long-term interest rates by i, and equity market returns by e. The data runs from 2024 to 2051.

Of foremost interest are the variations over time resulting from the scenarios and IAMs. The first three rows of fig. 1 show considerable differences in the impact that the policies have on GDP growth and inflation. Particularly the scenarios *Delayed Transition* and *Fragmented*

World, which impose substantial transition risks, lead to dips in GDP growth and inflation. The GDP growth rate slowly reverts, but inflation increases and remains higher thereafter for several years. The orderly scenarios *Net Zero 2050* and *Below* $2\,^{\circ}C$ in which immediate transitions take place show the opposite pattern with lower GDP growth but higher inflation in the years up to 2030. After 2030, the orderly scenarios have among the highest GDP growth and lowest inflation. The variation in impact between the scenarios is lowest in GCAM, followed by MESSAGEix and REMIND.

The different scenarios have a pronounced and stable effect on the long-run real interest rate. The orderly transitions in *Net Zero 2050* and *Below* $2\,^{\circ}C$ lead to quick technological advances reflected in high rates. In the *Delayed Transition* scenario, measures are postponed until after 2030, after which the real rate catches up with the former two. In the Hot house world of *NDCs* and *Current Policies*, physical risks remain high with a detrimental effect on productivity and technological advances, as signaled by a relatively low long-term real rate. The *Fragmented World* scenario shows a low rate until 2030 and modest increases thereafter. In GCAM and MESSAGEix, real rates remain different over the complete out-of-sample period, whereas they move closer together in REMIND.

The scenarios differ little in their effect on the equity market return. The *Delayed Transition* scenario leads to decreased stock returns lasting a few years after 2030. Particularly in the REMIND predictions, this decrease is sizeable, but it is followed by higher returns after 2035. The predictions for the relative changes in the oil price vary considerably over the scenarios and the IAMs as shown in fig. 1. MESSAGEix predicts large increases in the early years of the *Net Zero 2050* scenario with stable prices after 2032. REMIND predicts large and prolonged price increases in the *Delayed Transition* scenario after 2030. Whereas the differences between the scenarios become smaller in the predictions by MESSAGEix and REMIND toward the end of the out-of-sample period, they remain large in the GCAM predictions.

Together, the scenarios indicate quite different paths for the economy. On the one hand, the orderly transitions of *Net Zero 2050* and *Below* $2\,^{\circ}C$ lead to early damages in the form of lower economic growth, higher inflation and rising oil prices, but after 2035 the benefits increase. The *Delayed Transition* scenario is disorderly, with a sharp decrease in GDP growth and the equity market in the early 2030s. The initially low inflation rate increases substantially. The *Fragmented World* scenario shows similar but less extreme effects. In the hot house world scenarios of *NDCs* and *Current Policies*, measures are more limited, and consequently, all indicators show

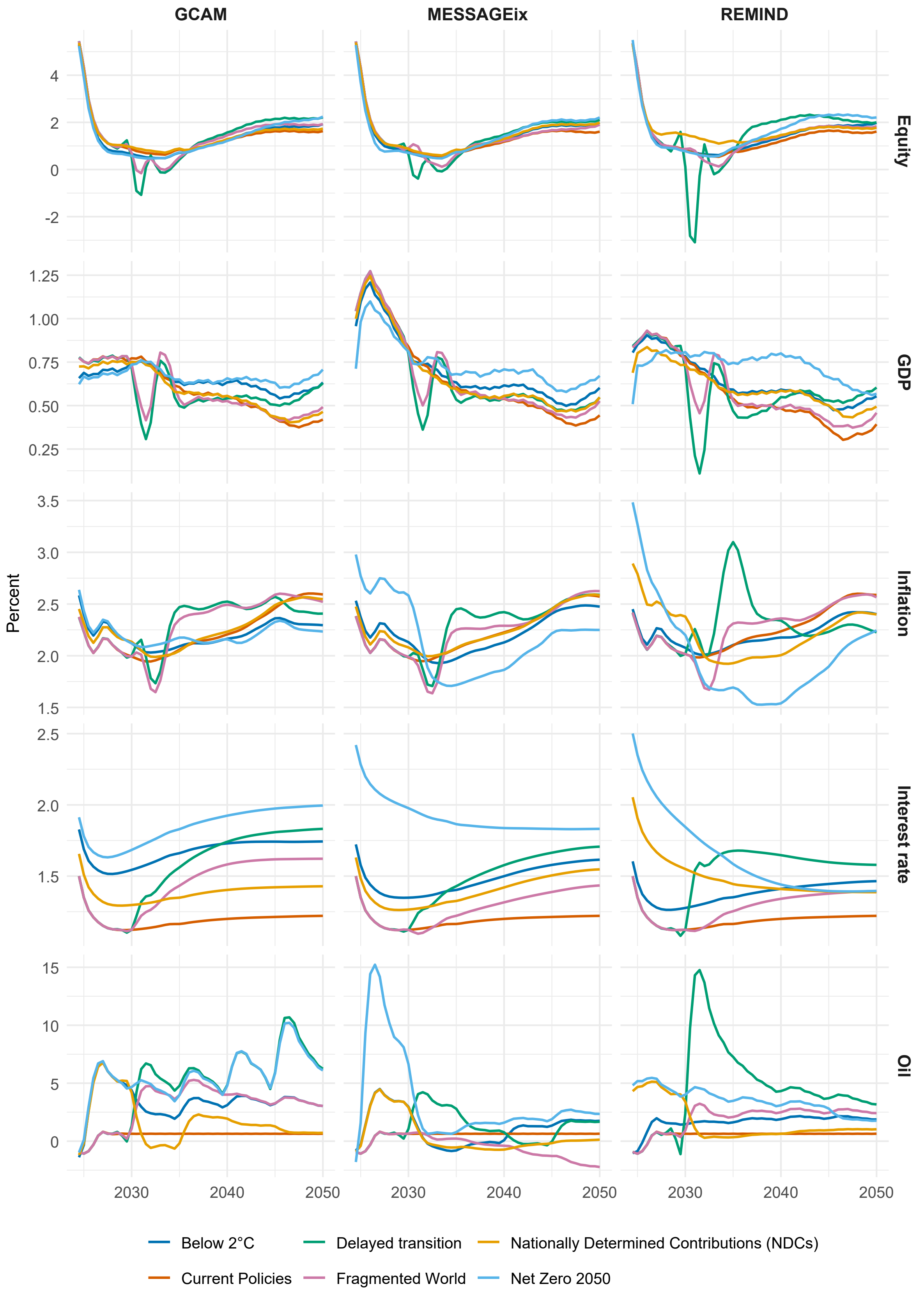

Figure 1: Predictions of the economic indicators in the NGFS scenarios
The figure presents predictions of the in the six different climate policies between 2024 and 2050. The rows correspond with the different economic indicators and the columns with the different IAMs; GCAM, and MESSAGEix and REMIND.

stable trajectories with a downward trend in economic growth and low long-term real interest rates.

The figures reveal that while the three models tend to deliver estimates that are qualitatively similar with respect to these economic variables, the magnitude of the effects can vary substantially. In particular, they provide very different assessments of the magnitude of effects from a delayed transition. The REMIND model tends to indicate more extreme effects. Furthermore, the effect on oil price changes (fig. 1) varies greatly over the models.

In all, the models and scenarios in the NGFS data provide a wide range of possible paths for the economic indicators. The differences across the scenarios in the economic variables of interest are substantial and indicate very different economic conditions. However, contrasting the transition risk models highlights some ambiguity regarding how severe the effects are expected to be in different scenarios. We do not take a stance on the likelihood or accuracy of these assessments but present results across all models.

4 Estimation results

We first present the estimates based on historical data. We begin with the estimates of the latent factors that capture commonalities in credit migrations. We then relate these factors to the economic indicators observed during the period and construct a linear model to track their changes.

4.1 Estimates of the latent credit factor

From the unconditional transition probabilities summarized in table 1, we obtain an estimate of the threshold matrix $\boldsymbol{K}$ as in eq. (17). We then proceed to estimate the factor exposures and the latent factors. We assume that the credit cycle is well approximated by a two-factor model. This specification is flexible enough to allow the cycle to vary across cohorts, while remaining suitably parsimonious relative to the available sample.

The estimation results are reported in table 4. By construction, the thresholds are decreasing across the destination cohort, that is, over the columns, indicating that a more negative realization of Y_{im} leads to a larger downgrade. They are increasing over the departure cohorts, that is, over the rows, which means that for a downgrade of, for example, a BBB-rated bond to B, a less negative realization of Y_{im} is needed than for an A-rated bond, as the threshold is -3.100 for A and -2.034 for BBB. This pattern in the data corresponds to economic logic, and does not arise by construction.

cohort	AAA-AA	A	BBB	BB	B–C	λ_1	λ_2	ρ_m
AAA–AA	−1.684	−2.588	−3.499	−3.606	−3.782	0.170	0.193	0.066
A	2.806	−1.813	−3.100	−3.283	−3.511	0.150	0.090	0.030
BBB	3.417	2.237	−2.034	−2.787	−3.307	0.209	0	0.044
BB	3.726	3.367	2.079	−1.661	−3.062	0.181	0.125	0.048
B–C	4.299	3.378	3.184	2.040	−2.178	0.096	0.236	0.065

Table 4: Estimation results for the CreditMetrics model with 2 factors

This table shows the estimates for the thresholds, the factor exposures and the resulting intra-cohort correlations in the CreditMetrics model specified in eqs. (1), (3) and (4). The columns labeled with a cohort give the estimates for the thresholds as in eq. (17). The columns labeled with λ_1 and λ_2 give the estimates for the factor exposures as in eq. (20). The intra-cohort correlations follow from the factor exposures, $\rho_m = \boldsymbol{\lambda}_m'\boldsymbol{\lambda}_m$. To identify the factors, we impose that λ_2 equals zero for the BBB cohort.

The estimates for the factor exposures show that the first factor can be interpreted as a level factor and the second one more as a curvature factor. The joint effect of the common factors is given by the intra-cohort correlation $\rho_m = \boldsymbol{\lambda}_m'\boldsymbol{\lambda}_m$, reported in the last column. These correlation parameters show a U-shape where the effect of the common factors is highest in the extreme cohorts AAA–AA and B–C. Since the variance of the latent credit indicator Y_{it} equals 1, the intra-cohort correlation also indicates how much of its variation is explained by the common factors. For the AAA–AA cohort this is largest at 6.6% and lowest for the A cohort at 3%. For identification, we impose that λ_2 equals zero for the BBB cohort, as this is one of the larger cohorts. Varying the identification restriction alters the exposure estimates ($\boldsymbol{\lambda}_m$) but does not affect the intra-cohort correlations (ρ_m).

We proceed to estimate the latent factors $\boldsymbol{F}_t$ and determine their joint effect $\lambda_m \boldsymbol{F}_t / \sqrt{\boldsymbol{\lambda}_m'\boldsymbol{\lambda}_m}$ for each cohort. Whereas the factors depend on the identification restriction, their joint effect is uniquely determined. Figure 2 reveals states of the corporate bond market that vary intuitively over time. We plot the number of upgrades and downgrades in each period on the secondary vertical axis. The credit cycle was low in the early 2000s, coinciding with the period of the dot-com bubble and its aftermath. It recovered until the financial crisis of 2008, which marked the lowest point in our sample. Following the financial crisis, we observe a period of better credit states, ultimately interrupted by the COVID-19 pandemic.

All cohort-factors are constructed such that they have approximately mean zero and variance 1, and follow the actual pattern in upgrades and downgrades quite closely. The graphs show mild heterogeneity over the cohorts. For example, the lowest cohort B–C, seems more strongly affected by the financial crisis of 2008, but less by the COVID-19 pandemic. Government support

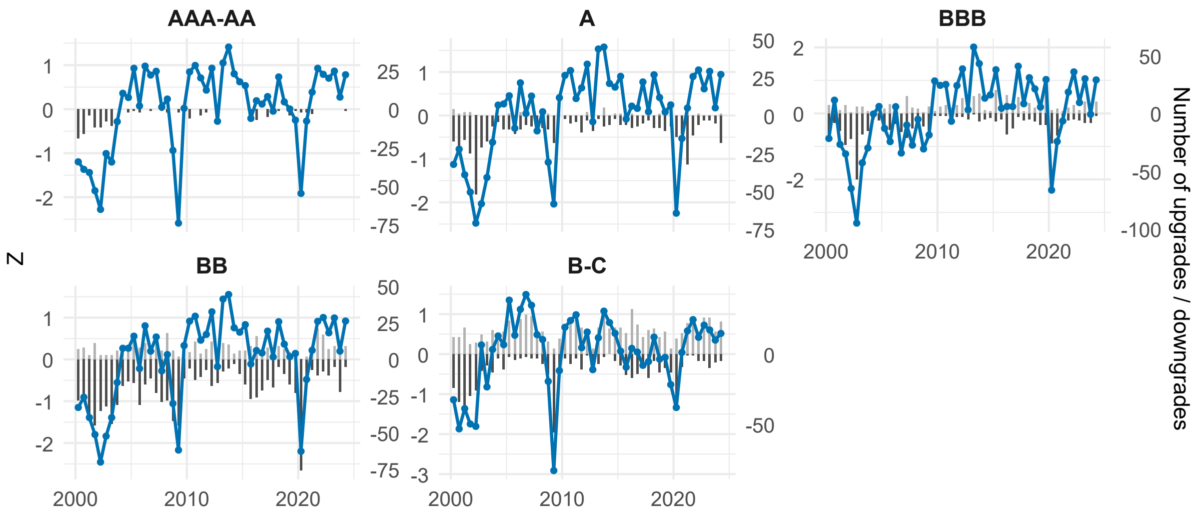

Figure 2: Joint effect of the latent factors estimates per cohort
The figure presents the estimated latent factors per cohort together with the upgrades and downgrades in each half-year period. We set the number of latent factors equal to 2. For each cohort, the joint effect of the latent factors follow as $Z_{mt} = \boldsymbol{\lambda}_m' \boldsymbol{F}_t / \sqrt{\boldsymbol{\lambda}_m' \boldsymbol{\lambda}_m}$ with estimates for $\boldsymbol{\lambda}_m$ reported in table 4. The factor estimates follow from eq. (21). The bars give the number of upgrades (light grey, positive) and downgrades (dark grey, negative) with the scale indicated on the secondary vertical axis.

during the pandemic may have prevented defaults but not downgrades of higher rated firms. Surprisingly, the BBB-cohort was not strongly affected by the financial crisis, as reflected by the small number of downgrades and consequently small negative values for its factor. This feature may be explained by the stickiness of the BBB cohort as the lowest investment grade cohort.

4.2 Relating changes in the factor to economic indicators

Using the economic indicators, we fit linear models to track changes in the credit cycle of each cohort. Table 5 presents the OLS estimates of the parameters in eq. (5) and table 6 presents the correlations of the dependent and independent variables. Because the COVID-19 period introduces significant outliers in the data, we exclude those two observations from the dataset. The correlation table reveals that the strongest univariate predictor differs across the cohorts. In the highest and lowest rated cohorts the respective cycles are most closely related to GDP growth, while in the remaining cohorts the real interest rate provides the highest univariate fit. The regression results in eq. (5) further show that in all cohorts, coefficients for the GDP growth rate and equity market return are positive, indicating conditionally positive relations with the credit cycle. In contrast, the real interest rate have a strong and negative effect on the credit cycles, as a higher rates increases the cost of borrowing (in real terms) and reduces economic growth. Changes in oil prices and the inflation rate only have marginal impacts on the credit

Table 5: Linear macro-finance models per cohort

	AAA–AA		A		BBB		BB		B–C	
g	0.25	0.23	0.19	0.17	0.03	0.02	0.20	0.18	0.30	0.29
	(0.16)	(0.06)	(0.14)	(0.11)	(0.15)	(0.13)	(0.15)	(0.11)	(0.13)	(0.08)
e	0.24	0.20	0.30	0.25	0.34	0.28	0.29	0.24	0.14	0.14
	(0.08)	(0.11)	(0.08)	(0.13)	(0.17)	(0.15)	(0.08)	(0.14)	(0.12)	(0.17)
i	−0.35	−0.09	−0.46	−0.17	−0.54	−0.34	−0.44	−0.15	−0.19	−0.02
	(0.17)	(0.05)	(0.14)	(0.08)	(0.14)	(0.08)	(0.14)	(0.08)	(0.23)	(0.10)
π	0.16	−0.05	0.13	−0.04	0.05	−0.02	0.13	−0.04	0.17	−0.02
	(0.13)	(0.09)	(0.14)	(0.13)	(0.23)	(0.19)	(0.14)	(0.13)	(0.15)	(0.10)
p	−0.12	0.10	−0.15	0.05	−0.17	−0.07	−0.14	0.06	−0.07	0.11
	(0.13)	(0.05)	(0.16)	(0.11)	(0.26)	(0.22)	(0.15)	(0.11)	(0.13)	(0.09)
Z_{t-1}		0.59		0.55		0.38		0.56		0.54
		(0.05)		(0.09)		(0.11)		(0.09)		(0.04)
ψ^2	0.64	0.46	0.57	0.51	0.55	0.64	0.58	0.49	0.73	0.51
R^2_{LOO}	0.27		0.33		0.20		0.32		0.09	

The table reports estimates from linear regressions of each cohort–factor Z_k onto economic variables and, for the dynamic specification, the first lag of the same factor. The cohort-factors are as constructed and reported in fig. 2. We denote GDP growth by g, inflation by π, oil price changes by p, long-term interest rates by i, and equity market returns by e. All economic indicators have been centered and the coefficients associated with the economic variables have been scaled such that they represent the change in the dependent variable resulting from a one-standard deviation increase in the corresponding predictor. Newey–West standard errors are reported in parentheses. The constrained residual variance is $\psi_m^2 = 1 - \phi_m^2 - \boldsymbol{\beta}_m \boldsymbol{\Sigma}_X \boldsymbol{\beta}_m$. The unconstrained R^2_{LOO} is computed as one minus the ratio of the unconstrained leave-one-out error variance to the unconstrained cohort–factor variance and is unavailable for dynamic specifications.

cycles once the other economic indicators are accounted for.

In the dynamic models, the AR coefficients tend to be substantial with values between 0.38 and 0.59. This indicates that shocks to the credit cycle are relatively persistent. While the estimated effects of GDP growth and equity returns are robust to the inclusion of the AR term, the coefficients associated with inflation, oil prices, and real interest rates are notably attenuated.

The values for the adjusted R^2 range from 0.23 to 0.40 for the static models indicate that the economic indicators explain a substantial part of the variation in the credit cycle. They also indicate that the joint fit of the variables is good, even though the standard errors are relatively large and indicate that some estimates are insignificant. Introducing an AR component leads to substantial increases in R^2 values up to 0.64 and lower standard errors.

In small samples, overfitting can be a significant concern. To obtain an estimate of the out-of-sample fit, we compute the linear fit of the economic variables using a leave-one-out approach.[11] Unsurprisingly, the values for the leave-one-out R^2 are lower than for the in-sample adjusted R^2, but they remain meaningful. Together, the results show that a linear combination

[11] Specifically, when we leave out the observation for time s and cohort m, we first construct the estimate $\hat{\boldsymbol{\beta}}_{ms}$ without this observation, and then construct the leave-one-out residual as $\hat{u}_{ms} = Z_{ms} - \hat{\boldsymbol{\beta}}'_{ms}\boldsymbol{X}_s$. The corresponding R^2_{LOO} for cohort m follows as $1 - \text{var}[\hat{u}_{ms}]/\,\text{var}[Z_{ms}]$, where $\text{var}[\hat{u}_{ms}]$ denotes the variance of the leave-on-out error series, and $\text{var}[Z_{ms}]$ the variance of the original series.

of the economic indicators provides an empirically relevant prediction of the credit cycle for each cohort. This holds in particular for the AAA–AA, A and BB cohorts, and is a bit weaker for the BBB and B–C cohorts.

Table 6: Correlation between latent factor estimates and economic indicators

	Z_{AAA-AA}	Z_A	Z_{BBB}	Z_{BB}	Z_{B-C}	r	i	g	π	p
Z_{AAA-AA}	1.00									
Z_A	0.94	1.00								
Z_{BBB}	0.64	0.86	1.00							
Z_{BB}	0.96	1.00	0.83	1.00						
Z_{B-C}	0.92	0.74	0.29	0.78	1.00					
e	0.41	0.42	0.35	0.42	0.33	1.00				
i	−0.46	−0.55	−0.57	−0.54	−0.28	−0.16	1.00			
g	0.47	0.39	0.18	0.41	0.49	0.46	−0.14	1.00		
π	0.30	0.21	0.02	0.23	0.36	0.16	0.00	0.58	1.00	
p	0.25	0.18	0.04	0.20	0.29	0.50	0.02	0.56	0.57	1.00

The table reports correlations between the credit cycle for each cohort $Z_{AAA-AA}, \ldots, Z_{B-C}$ and economic indicators during the in-sample period. We denote equity market returns as e, long-term interest rates as i, GDP growth as g, inflation as π, and oil price changes as p.

5 The impact of transition scenarios on credit risk

In this section, we combine the models for the credit cycles from the previous section with the NGFS scenarios. We employ these scenarios to make predictions of the credit cycles up to 2050 and use them to investigate the consequences for the risk profile of different bond portfolios. Increased risk implies that the amount of required economic capital increases, which we assume to translate proportionally into higher opportunity costs. To keep the exposition of the results clear, we focus our discussion on the risk management implications of the credit cycles obtained from the REMIND model. The results from the GCAM and MESSAGEix models are presented in Appendix B.4. The results are qualitatively similar across models.

5.1 Transition scenarios and the credit cycles

We present the predicted effects that a particular NGFS scenario has on the credit cycles in fig. 3. The predictions follow from eq. (5), starting from the last estimate of the factor realization Z_{mT}. Because the AR coefficients are substantial and the estimates for the last realization are positive for all cohorts, as shown in fig. 2, the first prediction, corresponding to the first half of 2025, is positive for all scenarios and cohorts. From the second prediction onward, the predictions diverge across scenarios and cohorts. Two periods are particularly critical: (1) the early period ending in 2030, during which orderly transition scenarios incur greater transition-related damages, and

(2) the period from 2030 to 2040, when disorderly transition scenarios incur greater damages.

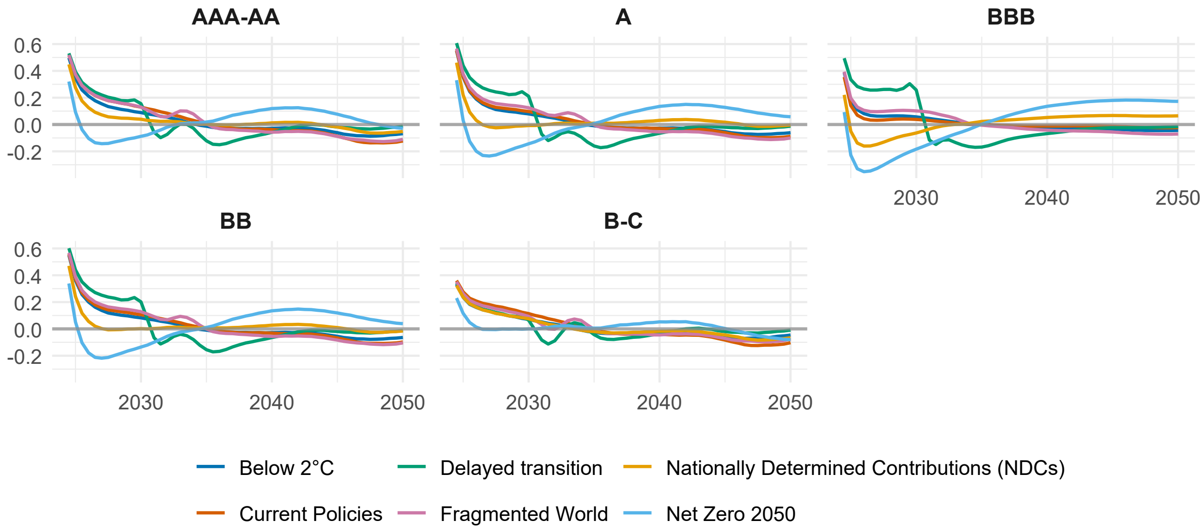

Figure 3: Predictions for the impact of transition scenarios on the credit cycle
The figure presents the predicted values of the credit cycle for the different cohorts under six different transition scenarios. Predictions are formed based on the model in eq. (5) with parameter estimates in table 5. The values of the economic indicators in the different scenarios are generated by the REMIND model. The predictions take the estimate for the last factor realization Z_{mT} as a staring point. They run from 2024 to 2050.

Figure 3 shows considerable variation in the impact of the different scenarios, and some variation in their impact for the different cohorts. Economic damages arising from transition risk in the orderly transition scenarios cause a rapid reversion from the high initial states. The impact of the *Net Zero 2050* scenario is especially severe, as the four highest cohorts (AAA–AA, A, BBB and BB) remain in negative states of the cycle until 2035. However, following the early-period damages, the credit cycles recover and, from 2035 onward, are predicted to be higher than those under the other transition scenarios. Our results indicate that the credit cycle of lowest rated assets (B–C) is generally less affected by the damages that occur due to transitional risk. A likely explanation lies in the effect of the long-term real interest rates on the credit cycle, which is much smaller in the B–C cohort than in all other cohorts (see Table 5).

In contrast to the *Net Zero 2050*, credit cycles remain high in the early period in all other transition scenarios but deteriorate after 2030. Scenarios with high physical risks, notably *Current Policies* and *Fragmented World*, produce a prolonged period of negative impacts after 2035. The *Delayed Transition* scenario produces particularly large negative effects in the early 2030s, from which credit cycles in the highest-rate cohorts recover only by the mid-2040s. The damages under the *Fragmented World* scenario are smaller than those predicted under the *Delayed Transition* scenario. However, damages from physical risk persist into later periods, leading to lower predicted credit cycles than in the other transition scenarios.

As such, it is clear that both physical risk and transition risk negatively impact the credit cycles of the bond cohorts that we consider. Transition risk tends to be large in magnitude but transitory, offsetting persistent physical risk in the later part of the sample. The *NDCs* scenario is somewhat anomalous in this regard. However, the qualitative results obtained for this scenario are not robust to the choice of IAM, as demonstrated in Appendix B.4.

5.2 Economic capital requirements per cohort

We next investigate the consequences for the economic capital requirements that regulated financial institutions must meet when holding these bonds. We interpret the effects of the different scenarios as a prediction of the conditional expected value of the credit cycle, and do not assume that the scenarios fully determine the realization of the cycle. In the calculation of the risk measures, we include this uncertainty about the cycle, meaning that they can be interpreted as largely through-the-cycle. We focus on well-diversified bond portfolios within a single cohort, based on the asymptotic results presented in section 2.2, and present results for heterogeneous portfolios in the next section. The effects on economic capital requirements are reported as percentage changes relative to a benchmark. Under the assumption that the opportunity costs associated with capital requirements change proportionally with their level, the percentage change can be directly interpreted as increases or decreases in costs.

Figure 4 shows the evolution of capital requirements for each cohort and transition scenario relative to the neutral state of the credit cycle. The high initial states of the cycles are maintained because of the substantial AR effect. As a result, initial capital requirements are higher under the neutral benchmark than under any transition scenario across all cohorts. As the effect of the initial state dissipates, economic capital in all scenarios increases.

The fastest increase in economic capital takes place in the *Net Zero 2050* scenario. For the four highest ranked cohorts, the economic capital exceeds the benchmark already in 2025 and peaks at around 20% higher than the benchmark. Around 2035, it is close to the neutral benchmark, and after 2035 it is generally 5 to 10% lower. To assess the economic significance of these effects, it is important to note that the reduction persists for roughly 15 years, leading to substantially lower aggregate opportunity costs.

The initially low capital requirement under the *Delayed Transition* scenario becomes very volatile when the transition starts in 2030. In this scenario, economic capital remains high during the period 2030–2040 and typically exceeds the economic capital resulting from other

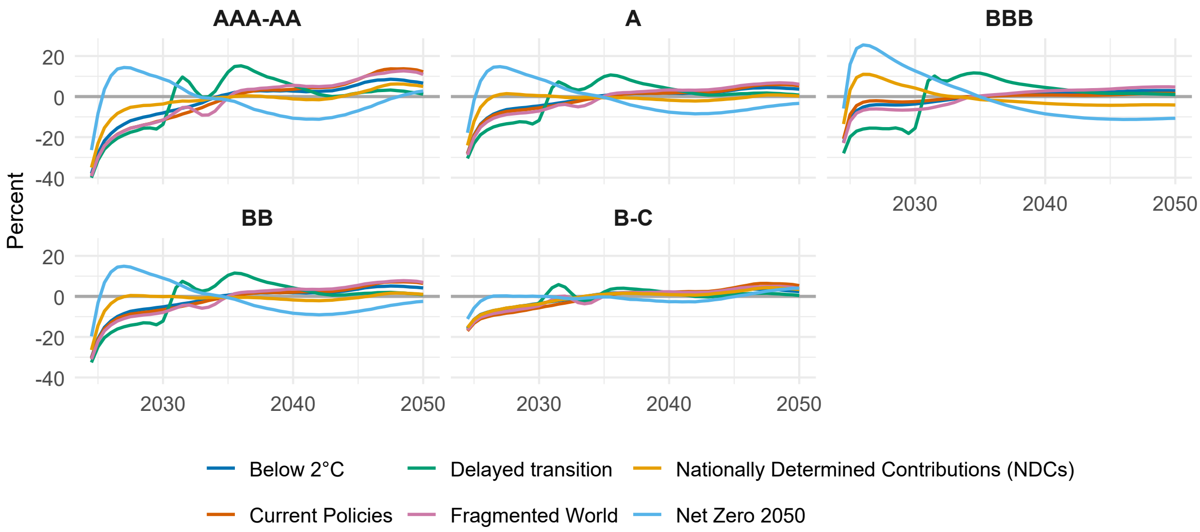

Figure 4: Economic capital relative to the neutral state

The figure presents the development of the predicted economic capital in the different transition scenarios as the percentage change relative to the neutral state of the credit cycle from 2024 to 2050. Economic capital is calculated as the difference between the 0.999 quantile and the expectation of the loss distribution conditional on the economic indicators and the prediction of the credit cycle in the previous period as given by eq. (13). The quantile follows from eq. (12) and the expectation from eq. (6). The values for μ_{mt} required in these expressions are as constructed and shown in fig. 3, and the values for σ_m are in table 5. The values for the economic indicators are generated using the REMIND model. The neutral state of the credit cycle assumes that the economic indicators and the previous prediction of the credit cycle are all at their long-term average and corresponds with $\mu_{mt} = 0$.

scenarios in that period. After 2040, the requirement returns to the levels of the benchmark and the other scenarios. In the other scenarios, we find that economic capital at the start of the scenarios increases faster than in *Delayed Transition* but not as fast as in *Net Zero 2050*. Instead of a volatile period followed by an improvement, these scenarios generally show steady increases in economic capital that end up well above the benchmark after 2040.

The results for the cohorts of BB and higher show some heterogeneity, where the spread between the scenarios is largest for the BBB-cohort in the period before 2035, and for the AAA-cohort in the period thereafter. The volatility in the *Delayed Transition* transition is highest for the AAA-cohort. The *NDCs* scenario leads to sharp increases for the BBB-cohort in the early period followed by a slow decrease, which is much less pronounced for the other cohorts. We conclude that the effects of the different scenarios are qualitatively similar for these four cohorts relative to the neutral credit state, though of course, in an absolute sense, the effect is a lot smaller for AAA–AA than for BB, as shown in fig. B.2 in the appendix.

The differences between scenarios and the neutral benchmark are smaller in the high-yield B–C cohort. However, here too, the *Net Zero 2050* scenario leads to the fastest increase in economic capital. The peak is now only slightly above the benchmark, after which economic capital drops to slightly below the benchmark. The volatility in economic capital resulting from the *Delayed*

Transition scenario is also less extreme than for the other cohorts. The other scenarios lead to steady increases in economic capital, though it deviates less from the benchmark. There are two reasons why the B–C cohort exhibits lower sensitivity to the scenarios. First, the results for the satellite model in table 5 show a smaller absolute effect of the real long-term interest rate, which shows large variation over the scenarios in fig. 1. The second reason is more mechanical. The threshold for default is less far out in the tail for lower-ranked bonds and, as shown in fig. B.2, economic capital for the lowest-ranked cohort is about 100 times higher than for the highest cohort. Changes in μ_{mt} lead to large absolute changes in economic capital in the B–C cohort. However, economic capital is similarly high under the benchmark, thus the relative changes are smaller. Put precisely, the partial derivative of EC_{α}^{as} with respect to μ_{mt} divided by EC_{α}^{as} is smaller in an absolute sense at smaller absolute values of $K_{q-1,m}$.

To directly compare the different transition scenarios to each other, we plot the change in economic capital using the *Current Policies* scenario as a benchmark in fig. 5. Of course, the ranking of the different scenarios by their effect on economic capital does not change, but the magnitude and evolution do.

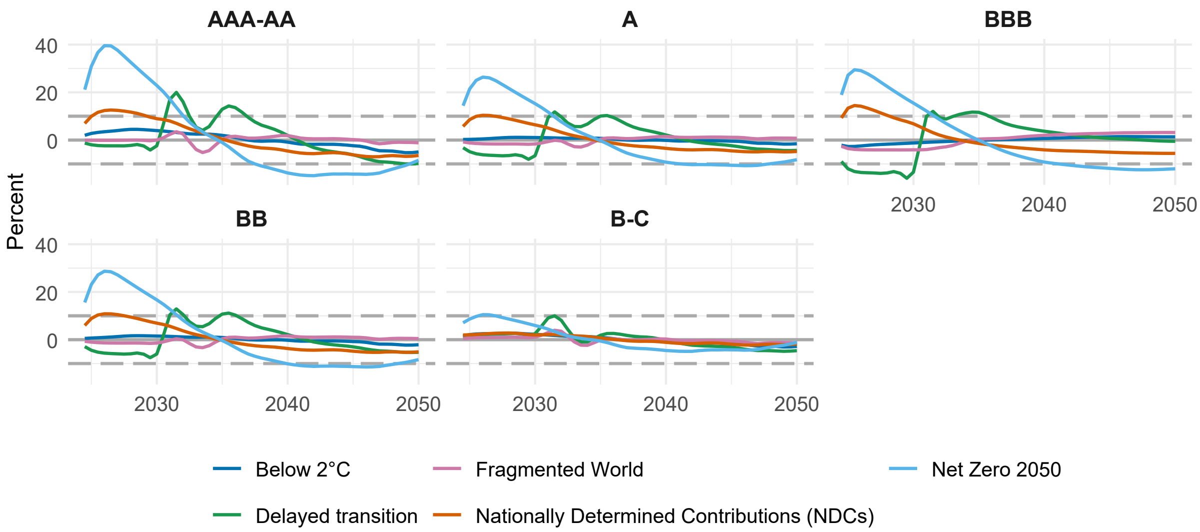

Figure 5: Changes in economic capital relative to *Current Policies*
The figure presents the development of the predicted economic capital in the different transition scenarios as the percentage change relative to the *Current Policies* scenario level from 2024 to 2050. Economic capital is calculated as the difference between the 0.999 quantile and the expectation of the loss distribution conditional on the economic indicators and the prediction of the credit cycle in the previous period as given by eq. (13). The quantile follows from eq. (12) and the expectation from eq. (6). The values for μ_{mt} required in these expressions are as constructed and shown in fig. 3, and the values for ψ_m are in table 5. The values for the economic indicators are generated using the REMIND model. The dashed (gray) line provide reference lines at 10 and -10 percent.

For the AAA–AA to BB cohorts, the *Net Zero 2050* scenario leads to increases in economic capital of over 20% in the first five years, with a peak between 30 and 40%. After 2035, however, economic capital is around 10% lower than in the *Current Policies* benchmark. The disorderly *Delayed Transition* scenario initially leads to lower economic capital, although not much below the benchmark. During the volatile period starting in 2030, required capital reaches levels 10 to 20% higher than expected under *Current Policies*, after which capital requirements fall below the benchmark after 2040. The *Fragmented World* scenario does not differ much from the benchmark, whereas the *NDCs* scenario leads to initially higher economic capital followed by lower values later on, although deviations from the benchmark are more modest in both directions compared to the *Net Zero 2050* scenario.

Using *Current Policies* as a benchmark puts the effects of the different scenarios on economic capital for the B–C cohort into different perspective. Compared to *Current Policies*, the *Net Zero 2050* scenario leads to higher economic capital up to 2035 with a maximum increase of about 10% followed by around 5% lower capital up to 2050. The other scenarios all lead to economic capital that starts slightly above the benchmark and then decreases to slightly below it, with a period with modest volatility between 2030 and 2035 in the *Delayed Transition* scenario.

In sum, our results highlight that the different transition scenarios carry pronounced implications for the risk profile of bonds and consequently also affect the capital requirements for financial institutions. Scenarios in which physical risks are lower lead to a persistent reduction in risk, and hence produce a prolonged period of lower capital requirements. All transition policies entail costs, and earlier implementation of measures leads to an earlier increase but also an earlier decrease in capital requirements. Scenarios in which there is less coordination, such as *Delayed Transition* and *Fragmented World* lead to substantial time variation in the risk measures. In practice, the timing in particular these scenarios may be quite uncertain, leading to higher capital requirements for a long period.

Importantly, we find stronger relative effects for investment-grade bonds than for the B–C cohort. Investment-grade bonds show on the one hand larger exposures to the business cycle, but part is also explained by the lower values of benchmarks. However, if a risk budget is fixed, relative effects give the relevant comparison. This means that tilting investments to higher ranked bonds does not reduce exposure to climate risk.

5.3 Heterogeneous bond portfolios

The results in the previous subsection apply to a portfolio with infinitely many equally weighted bonds in a specific cohort. In this subsection, we investigate the case of a portfolio with a fixed number of bonds with different weights and credit quality. We determine the risk profile of an investment-grade portfolio and a high-yield portfolio, both consisting of 2,000 bonds. The investment-grade portfolios has 25%, 50% and 25% in cohorts AAA-AA, AA and BBB, whereas the high-yield portfolio has 50% in BB and 50% in B–C. In the event of default, we assume a random exposure drawn from a uniform distribution between 1 and 50. Because the quantiles of the loss distributions for these portfolios are not available in closed form, we use Monte Carlo simulations using 10^7 iterations of random normal draws for $\tilde{\boldsymbol{u}}_t$ and $\tilde{\varepsilon}_{imt}$ as discussed in section 2.2.

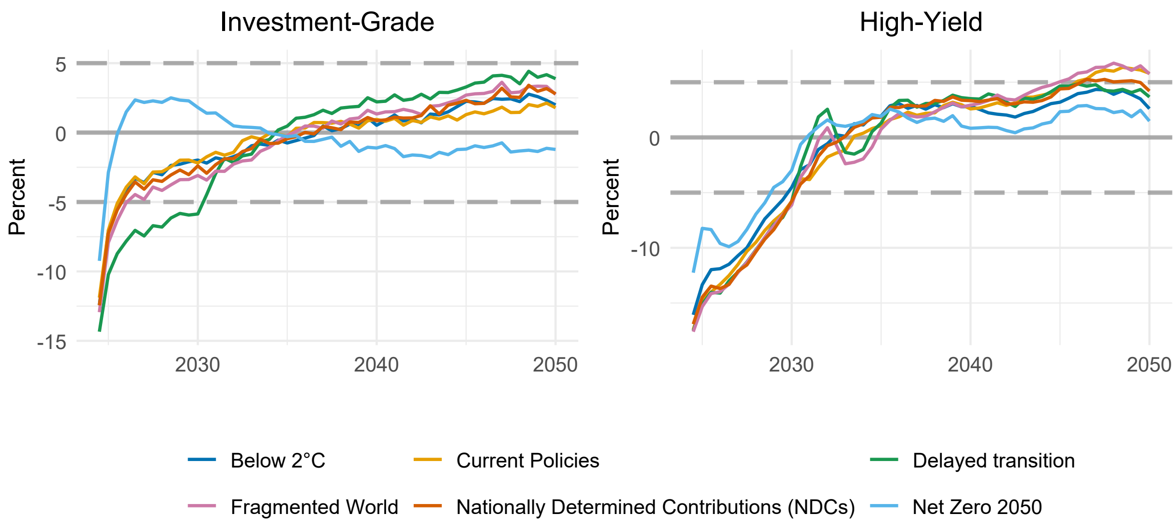

Figure 6: Changes in economic capital for heterogeneous bond portfolios relative to the neutral state.

The figure presents the development of the economic capital of an investment-grade and high-yield portfolio of bonds in the different policies as the percentage change relative to the neutral state of the the credit cycle from 2024 to 2050. The portfolios contain 2,000 assets each. In the investment-grade portfolio they are distributed 25% in AAA–AA, 50% in A, and 25% in BBB, and in the high-yield portfolios 50% in B and 50% are B–C. Economic capital is calculated as the difference between the 0.999 quantile and the expectation of the loss distribution conditional on the economic indicators and the prediction of the credit cycle in the previous period as given by eq. (13). The quantile is taken from the simulated loss distribution based on 10^7 iterations of random normal draws for $\tilde{\boldsymbol{u}}_t$ and $\tilde{\varepsilon}_{imt}$ in (2.2). The expectation follows from eq. (6). The values for μ_{mt} required in these expressions are as constructed and shown in fig. 3, and the values for ψ_m are in table 5. The exposure-at-default is drawn from a uniform distribution between 1 and 50 and the loss-given-default is equal to 1. The values for the economic indicators are generated using the REMIND model. The dashed (gray) line provide reference lines at 5 and -5 percent.

Figure 6 presents the development of economic capital for the different scenarios relative to the neutral credit state. The results for the investment-grade portfolio mix the results for the three constituent cohorts in fig. 4. The *Net Zero 2050* scenario leads to rapid increases in economic capital, putting it above the benchmark, followed by decreases that bring it below the benchmark. The *Delayed Transition* scenario keeps economic capital below the benchmark until 2035 but it leads to the highest economic capital thereafter. The other scenarios are in between and are characterized by a steady, prolonged increase in economic capital. However, an important difference is the magnitude of the changes, which falls within a range of -5 to +5% for most of the period. This magnitude is smaller because the presence of idiosyncratic risk increases the benchmark and reduces the relative effect of transition and physical risks on total risk.

The results for the high-yield portfolio are mostly driven by the bonds in the B–C cohort, as its level of economic capital is about 10 times higher than that for the BB cohort. So, as already observed in fig. 4, in all scenarios the economic capital starts favorably below the benchmark, moves close to it between 2030 and 2035 and exceed it thereafter. Differences between the scenarios are small, but the volatility resulting from the *Delayed Transition* and *Fragmented World* scenarios remains clearly visible. Compared to investment grade, all scenarios end up with higher economic capital than the benchmark, including the *Net Zero 2050* scenario, although its implied economic capital is lower than that under the other scenarios.

To contrast the transition scenarios, we again present economic capital relative to the level implied by the *Current Policies* scenario in Figure 7. The *Net Zero 2050* and *Delayed Transition* scenarios still stand out. The elevated transition risk in the *Net Zero 2050* scenario leads to higher economic capital in the first years of the prediction period. For the investment-grade portfolio, economic capital is approximately 2.5 percent higher than under *Current Policies*, with a peak of 6%, whereas for the high-yield portfolio it is at most about 7.5% higher. Similarly, the *Delayed Transition* scenario is associated with sharp and volatile increases in capital requirements around the transition period in the early 2030s, reaching up to 5 percent above *Current Policies* for the high-yield portfolio. For the investment-grade portfolio, the *Net Zero 2050* scenario leads to economic capital that stabilizes at 2.5% to 3.0% below the *Current Policies* scenario, while the other scenarios lead to economic capital requirements that exceed those in the *Current Policies* scenario by 2050. For the high-yield portfolio, all scenarios show declining economic capital requirements compared to *Current Policies*, ending below this benchmark. This pattern is most pronounced for the *Net Zero 2050* scenario but present for all except for the *Fragmented World* scenario.

We conclude that, physical and transition risks remain economically meaningful for credit risk even in smaller portfolios composed of assets from different cohorts. The effects are smaller than for homogeneous asymptotic portfolios, and differences between scenarios are less pronounced, but we still observe that the *Net Zero 2050* scenario pairs higher risk early on with substantial

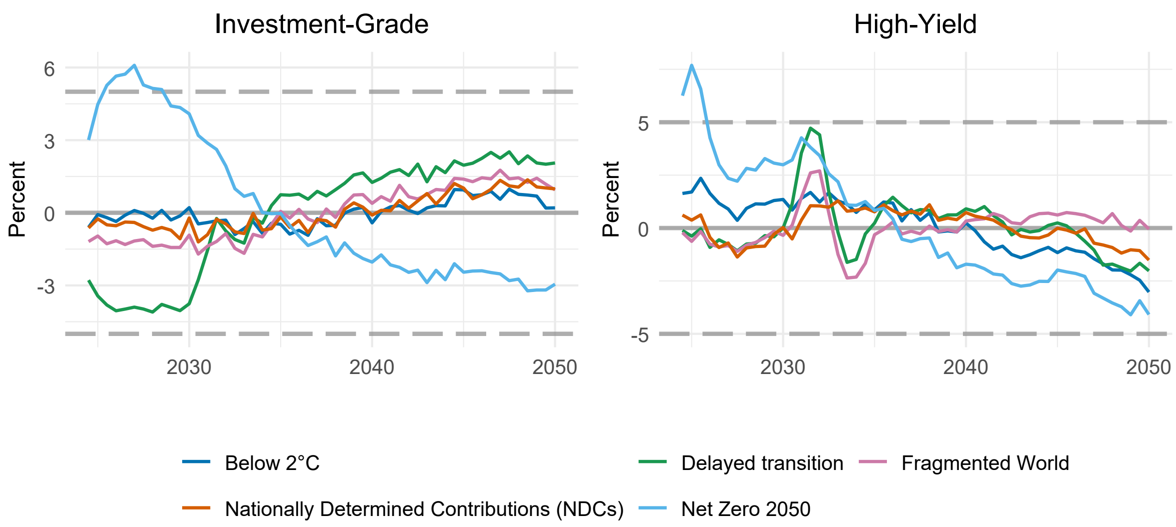

Figure 7: Changes to economic capital for heterogeneous bond portfolios relative to the *Current Policies* scenario
The figure presents the development of the economic capital of an investment-grade and high-yield portfolio of bonds in the different policies as the percentage change relative to the *Current Policies* scenario from 2024 to 2050. The portfolios contain 2,000 assets each. In the investment-grade portfolio they are distributed 25% in AAA–AA, 50% in A, and 25% in BBB, and in the high-yield portfolios 50% in B and 50% are B–C. Economic capital is calculated as the difference between the 0.999 quantile and the expectation of the loss distribution conditional on the economic indicators and the prediction of the credit cycle in the previous period as given by eq. (13). The quantile is taken from the simulated loss distribution based on 10^7 iterations of random normal draws for $\tilde{\boldsymbol{u}}_t$ and $\tilde{\varepsilon}_{imt}$ in (2.2). The expectation follows from eq. (6). The values for μ_{mt} required in these expressions are as constructed and shown in fig. 3, and the values for ψ_m are in table 5. The exposure-at-default is drawn from a uniform distribution between 1 and 50 and the loss-given-default is equal to 1. The values for the economic indicators are generated using the REMIND model. The dashed gray lines indicate reference levels at $\pm 5\%$.

decreases over a prolonged period thereafter. The *Delayed Transition* scenario postpones the increase in risk but creates a five-year period of volatility, followed by a period during which costs remain above the considered benchmarks. For the high-yield portfolio, the *Current Policies* scenario eventually leads to the highest costs, whereas this is the case for *Delayed Transition* in the investment-grade portfolio.

5.4 Results for the other IAMs

We repeat the analyses of the previous subsections using the GCAM and MESSAGEix as alternatives to REMIND as Integrated Assessment Model. We focus on the similarities and differences relative to our main findings. The full set of results is available in appendix B.4.

Using GCAM leads to smaller differences between the different transition scenarios. For all cohorts, the credit cycles start favorably but revert to the neutral values soon. The cycles remain slightly positive until around 2035 for all scenarios, including the *Net Zero 2050* scenario. The only exception is the B–C cohort where the credit cycle becomes negative for the *Delayed Transition* and *Fragmented World* scenarios already after 2030. This pattern translates into economic capital that generally remains lower than the neutral state until 2035, and becomes higher than it thereafter. The difference between the best and worst scenarios is at most 10 percentage points.

Comparing the economic capital in the different scenarios relative to the *Current Policies* scenario yields some further insights. Relative to *Current Policies*, the *Net Zero 2050* and *Below* $2\,^{\circ}C$ scenarios show the earliest increase in economic capital to levels (slightly) above this benchmark. After 2040, both scenarios fall below the benchmark. The *Below* $2\,^{\circ}C$ scenario shows smaller deviations from the benchmark than *Net Zero 2050*, which corresponds with this scenario involving less transition risk but also achieving smaller reductions in physical risk. The *NDCs* scenario produces economic capital values close to the benchmark. The *Delayed Transition* and *Fragmented World* scenarios lead to volatile predictions for economic capital that start below the benchmark and only drop below it at the end of the prediction window, or, in case of the BBB cohort, not at all.

The predictions for the credit cycles in the different transition scenarios resulting from the MESSAGEix model look more similar to those from the REMIND model. The *Net Zero 2050* scenario stands out again with a rapid deterioration of the credit state, though the subsequent improvement is less pronounced. The *Delayed Transition* scenario again maintains a favorable credit state for the longest period, but leads to less volatility between 2030 and 2035 than resulting from the REMIND model. The *Net Zero 2050* scenario shows the most favorable credit state after 2035 and is also the only one that remains positive or only slightly negative until 2050. These patterns are mirrored in the economic capital relative to the neutral state.

The comparison with *Current Policies* as a benchmark confirms our results for the *Net Zero 2050* scenario: required capital above this benchmark until 2035, but below it thereafter. The *Below* $2\,^{\circ}C$ scenario is also first above this benchmark and around or below it after 2040 for most cohorts. Here, too, we find that the *Delayed Transition* scenario leads to EC below the benchmark until 2030. Between 2030 and 2035, *Delayed Transition* and *Fragmented World* lead to similar swings in economic capital. Using the MESSAGEix, these two scenarios lead to higher economic capital than *Current Policies* for the AAA–AA to BB cohorts, whereas the REMIND model places them below the benchmark. The MESSAGEix results for the B–C cohort closely resemble those from REMIND.

In all, the results obtained using the other IAMs reinforce our main results from the previous sections. While the increased transition risk associated with orderly transitions impacts the risk profiles of the bond portfolios, the long-term reduction in physical risk offsets this increase by 2050.

6 Conclusion

In this paper, we assess how different transition scenarios affect the credit risk of corporate bonds. We propose a two-factor framework that is directly linked to key economic variables, allowing us to trace credit cycles through 2050 using NGFS projections. The latent risk factors that drive credit cycles across rating cohorts govern rating migrations and have immediate implications for the risk management and capital requirements of institutions holding corporate bonds.

We apply our framework to evaluate capital requirements for well-diversified portfolios within a single rating cohort and for portfolios with a finite number of bonds distributed across cohorts. We find that economic damages arising from physical and transition risks affect cohorts differently. Orderly transitions tend to cause short-term disruptions in credit cycles across most cohorts, but they mitigate the physical damages that would otherwise lead to deterioration. Delayed and disorderly transitions, in contrast, generate substantial transition-related deterioration and higher volatility due to abrupt adjustments. Finally, insufficient mitigation yields hothouse-world scenarios in which credit cycles are persistently weakened by severe projected physical damages.

Differences in credit-cycle dynamics translate directly into differences in the capital requirements financial institutions must satisfy to maintain well-diversified corporate bond portfolios. We find that variation in the conditional expectations of credit cycles produces sizable differences in required economic capital and, consequently, in the opportunity costs faced by regulated financial institutions. Because capital requirements move with the credit cycle, our results highlight a clear trade-off: orderly transitions generate short-term increases in opportunity costs but ultimately reduce them by lowering long-run physical risk. Over a 25-year horizon, the orderly transition aligned with the *Net Zero 2050* pathway more than compensates for early transition damages, leaving investors with lower capital requirements by the late 2040s relative to a continuation of current policies. In particular, we find that the cohort of highest-rated bonds is, in relative terms, highly exposed to the transition scenarios we consider.

Our study has several limitations. We focus exclusively on how climate-related economic damages affect the systemic risk of credit markets and associated capital requirements, omitting channels through which credit market dynamics may themselves influence the broader economy. Such feedback effects could amplify the impact of physical and transition risks. Moreover, we do not quantify the uncertainty surrounding our estimates of capital requirements and opportunity costs. A full treatment of this uncertainty is beyond the scope of this paper, as we treat NGFS scenario paths as exogenous inputs and do not account for the estimation uncertainty underlying those projections.

References

Acharya, V. V., Berner, R., Engle, R., Jung, H., Stroebel, J., Zeng, X. and Zhao, Y. (2023). Climate stress testing. *Annual Review of Financial Economics*, *15*(1), 291–326. doi: 10.1146/annurev-financial-110921-101555

Acharya, V. V., Johnson, T., Sundaresan, S. and Tomunen, T. (2022, September). *Is physical climate risk priced? Evidence from regional variation in exposure to heat stress.* NBER Working paper 30445. doi: 10.3386/w30445

Bansal, R., Kiku, D. and Ochoa, M. (2019, October). *Climate change risk.* Working paper, Duke University. Retrieved from `https://people.duke.edu/~rampini/BansalKikuOchoa2019.pdf`

Baudino, P. and Svoronos, J.-P. (2021, July). Stress-testing banks for climate change. In *FSI insights on policy implementation* (Vol. 34). [Basel]: Bank for International Settlements, Financial Stability Institute.

BCBS. (2005). *An Explanatory Note on the Basel II IRB Risk Weight Functions.*

BCBS. (2017). *Basel III: Finalising Post-crisis Reforms.*

BCBS. (2021, April). *Climate related risk drivers and their transmission channels.* Basel Committee on Banking Supervision, Bank for International Settlements, Basel, Switzerland. Retrieved from `https://www.bis.org/bcbs/publ/d517.htm`

Belkin, B., Suchower, S. J. and Forest Jr., L. R. (1998). A one-parameter representation of credit risk and transition matrices. *CreditMetrics Monitor*, *1*(3), 46-58.

Borio, C., Drehmann, M. and Tsatsaronis, K. (2014, June). Stress-testing macro stress testing: Does it live up to expectations? *Journal of Financial Stability*, *12*, 3–15. doi: 10.1016/j.jfs.2013.06.001

Carlehed, M. and Petrov, A. (2012, September). A methodology for point-in-time–through-the-cycle probability of default decomposition in risk classification systems. *The Journal of Risk Model Validation*, *6*(3), 3–25. doi: 10.21314/jrmv.2012.091

Cochrane, J. H. (2005). *Asset pricing* (Revised ed.). Princeton, New Jersey, US: Princeton University Press.

Cosemans, M., Hut, X. and Van Dijk, M. (2021). The impact of climate change on optimal asset allocation for long-term investors. *Netspar industry series*, *173*.

Creal, D., Schwaab, B., Koopman, S. J. and Lucas, A. (2014, December). Observation-driven mixed-measurement dynamic factor models with an application to credit risk. *The Review of Economics and Statistics*, *96*(5), 898–915. doi: 10.1162/REST_a_00393

Duffie, D., Eckner, A., Horel, G. and Saita, L. (2009, September). Frailty correlated default. *The Journal of Finance*, *64*(5), 2089–2123. doi: 10.1111/j.1540-6261.2009.01495.x

ECB. (2022, July). *2022 climate risk stress test* (Tech. Rep.). European Central Bank, Frankfurt, Germany. Retrieved from `https://data.europa.eu/doi/10.2866/97350` doi: 10.2866/97350

FED. (2024, May). *Pilot climate scenario analysis exercise* (Tech. Rep.). Board of Governors of the Federal Reserve System. Retrieved from `https://www.federalreserve.gov/publications/files/csa-exercise-summary-20240509.pdf`

Frye, J. (2000, November). Depressing recoveries. *Risk*, 108–111.

Giglio, S., Kelly, B. and Stroebel, J. (2021, November). Climate finance. *Annual Review of Financial Economics*, *13*(1), 15–36. doi: 10.1146/annurev-financial-102620-103311

Giglio, S., Maggiori, M., Rao, K., Stroebel, J. and Weber, A. (2021, March). Climate change and long-run discount rates: Evidence from real estate. *The Review of Financial Studies*, *34*(8), 3527–3571. doi: 10.1093/rfs/hhab032

Gordy, M. B. and Heitfield, E. (2010, June). Small-sample estimation of models of portfolio credit risk. In M. Kijima, C. Hara, K. Tanaka and Y. Muromachi (Eds.), *Recent advances in financial engineering 2009: Proceedings of the kier-tmu international workshop on financial engineering 2009.* World Scientific. doi: 10.1142/9789814304078_0002

Gupton, G. M., Finger, C. C. and Bhatia, M. (1997, April). *Creditmetrics — technical document.*

Javadi, S. and Masum, A. (2021, August). The impact of climate change on the cost of bank loans. *Journal of Corporate Finance*, *69*, 102019. doi: 10.1016/j.jcorpfin.2021.102019

Jung, H., Santos, J. A. C. and Seltzer, L. (2023, April). *U.S. banks' exposures to climate transition risks.* Federal Reserve Bank of New York Staff Reports, no. 1058.

Keijsers, B., Diris, B. and Kole, E. (2018). Cyclicality in losses on bank loans. *Journal of Applied Econometrics*, *33*, 533–552. doi: 10.1002/jae.2612

Klusak, P., Agarwala, M., Burke, M., Kraemer, M. and Mohaddes, K. (2023, December). Rising temperatures, falling ratings: The effect of climate change on sovereign creditworthiness. *Management Science*, *69*(12), 7468–7491. doi: 10.1287/mnsc.2023.4869

Koopman, S. J. and Lucas, A. (2008, October). A non-gaussian panel time series model for estimating and decomposing default risk. *Journal of Business & Economic Statistics*, *26*(4), 510–525. doi: 10.1198/073500108000000051

Koopman, S. J., Lucas, A. and Monteiro, A. (2008, January). The multi-state latent factor intensity model for credit rating transitions. *Journal of Econometrics*, *142*(1), 399–424. doi: https://doi.org/10.1016/j.jeconom.2007.07.001

Koopman, S. J., Lucas, A. and Schwaab, B. (2012, October). Dynamic factor models with macro, frailty, and industry effects for u.s. default counts: The credit crisis of 2008. *Journal of Business & Economic Statistics*, *30*(4), 521–532. doi: 10.1080/07350015.2012.700859

McNeil, A. J. and Wendin, J. P. (2007, March). Bayesian inference for generalized linear mixed models of portfolio credit risk. *Journal of Empirical Finance*, *14*(2), 131–149. doi: 10.1016/j.jempfin.2006.05.002

Merton, R. C. (1974). On the pricing of corporate debt: The risk structure of interest rates. *Journal of Finance*, *29*, 449–470.

Miu, P. and Ozdemir, B. (2006). Basel requirement of downturn LGD: Modeling and estimating PD & LGD correlations. *Journal of Credit Risk*, *2*(2), 43–68.

NGFS. (2024a, November). *NGFS Climate Scenarios Database: Technical Documentation V5.0.* `https://www.ngfs.net/system/files/2025-01/NGFSClimateScenariosTechnicalDocumentation.pdf`.

NGFS. (2024b, November). *NGFS climate scenarios for central banks and supervisors - phase V.* Report, Network of Central Banks and Supervisors for Greening the Financial System. Retrieved from `https://www.ngfs.net/en/publications-and-statistics/publications/ngfs-climate-scenarios-central-banks-and-supervisors-phase-v`

Painter, M. (2020, February). An inconvenient cost: The effects of climate change on municipal bonds. *Journal of Financial Economics*, *135*(2), 468–482. doi: 10.1016/j.jfineco.2019.06.006

Pfeuffer, M., Nagl, M., Fischer, M. and Rösch, D. (2020, April). Parameter estimation, bias correction and uncertainty quantification in the Vasicek credit portfolio model. *The Journal of Risk*, *22*(4), 1-30. doi: 10.21314/jor.2020.429

Reinders, H. J., Schoenmaker, D. and van Dijk, M. (2023, March). A finance approach to climate stress testing. *Journal of International Money and Finance*, *131*, 102797. doi: 10.1016/j.jimonfin.2022.102797

Reinders, H. J., Schoenmaker, D. and van Dijk, M. (2025, March). Climate risk stress testing: A critical survey and classification. *Journal of Climate Finance*, *10*, 100061. doi: 10.1016/j.jclimf.2025.100061

Roger, S. and Vlcek, J. (2012, January). *Macrofinancial modeling at central banks: Recent developments and future directions.* (IMF Working Paper 12/21)

Schuermann, T. (2004, February). What Do We Know About Loss Given Default? In D. Shimko (Ed.), *Credit risk models and management* (2nd ed., chap. 9). Risk Books, London.

Schwaab, B., Koopman, S. J. and Lucas, A. (2016, April). Global credit risk: World, country and industry factors. *Journal of Applied Econometrics*, *32*(2), 296–317. doi: 10.1002/jae.2521

Seltzer, L., Starks, L. and Zhu, Q. (2022, April). *Climate regulatory risk and corporate bonds.* (NBER Working paper 29994) doi: 10.3386/w29994

Stock, J. and Watson, M. (2016). Dynamic factor models, factor-augmented vector autoregressions, and structural vector autoregressions in macroeconomics. In J. B. Taylor and H. Uhlig (Eds.), *Handbook of macroeconomics* (Vol. 2, pp. 415–525). Elsevier. doi: 10.1016/bs.hesmac.2016.04.002

Stroebel, J. and Wurgler, J. (2021, November). What do you think about climate finance? *Journal of Financial Economics*, *142*(2), 487–498. doi: 10.1016/j.jfineco.2021.08.004

Vasicek, O. A. (1991). *Limiting Loan Loss Probability Distribution, KMV Working Paper.*

Vasicek, O. A. (2002). The distribution of loan portfolio value. *Risk*, *15*, 160–162.

Yang, B. H. (2014, September). Modeling systematic risk and point-in-time probability of default under the Vasicek asymptotic single risk factor model framework. *The Journal of Risk Model Validation*, *8*(3), 33–48. doi: 10.21314/jrmv.2014.126

Supplementary Material

A Derivation of the asymptotic portfolio loss distribution

To derive eq. (11), we first write the probability of default as a function of η_t for given values of $\boldsymbol{X}_t$ and Z_{t-1},

$$p_{qm}(\eta_{mt}; \boldsymbol{X}_t, Z_{m,t-1}) = \Pr[Y_{imt} \leq K_{q-1,m} | \eta_{mt}, \boldsymbol{X}_t, Z_{m,t-1}] = \Phi\left(\frac{K_{q-1,m} - \mu_{mt} - \sqrt{\rho_m}\psi_m\eta_t}{\sqrt{1-\rho_m}}\right), \tag{A.1}$$

with $\mu_{mt} = \sqrt{\rho_m}(\boldsymbol{\beta}_m' X_t + \phi_m Z_{m,t-1})$ following the second case in eq. (7). Consequently, the distribution of the percentage loss $\delta_{mt} = \lim_{N_{mt}\to\infty} \delta(N_{mt})$ follows as

$$\begin{aligned}\Pr[\delta_{mt} \leq v] &= \Pr[p_{qm}(\eta_{mt}; \boldsymbol{X}_t, Z_{m,t-1}) \leq v] = \Pr[\eta_{mt} \geq p_{qm}^{-1}(v; \boldsymbol{X}_t, Z_{m,t-1})] \\ &= \Phi(-p_{qm}^{-1}(v; \boldsymbol{X}_t, Z_{m,t-1}) = \Phi\left(\frac{\sqrt{1-\rho_m}\Phi^{-1}(v) + \mu_{mt} - K_{q-1,m}}{\sqrt{\rho_m}\psi_m}\right),\end{aligned} \tag{A.2}$$

where p_{qm}^{-1} denotes the inverse of $p_{qm}(\eta_{mt}; \boldsymbol{X}_t, Z_{m,t-1})$ as a function of η_{mt}, treating $\boldsymbol{X}_t, Z_{m,t-1}$ as parameters, which is a monotonically decreasing. This result differs from Vasicek (1991), as some conditional information of the realization of the common factor is known, leading to an additional term μ_{mt} in the numerator and a reduction of the denominator by a factor ψ_m.

B Additional data analysis

B.1 Capital Requirement Regulation

The Capital Requirements Regulation (CRR) is a key EU regulation that sets prudential requirements for banks. It is closely linked to the Capital Requirements Directive and is the EU's direct implementation of the Basel framework. Under the standardised approach for credit risk, the regulation assigns risk weights to corporate debt exposures based on their external credit ratings (Table 7). This mapping is based on the European Banking Authority's mapping of External Credit Assessment Institutions to the credit quality steps defined in the CRR as of January 1, 2025.[12]

Table 7: Mapping of S&P credit ratings to credit quality steps and risk weights.

	S&P rating									
	AAA	AA	A	BBB	BB	B	CCC	CC	C	$R/SD/D$
Risk weight (%)	20	20	50	75	100	150	150	150	150	150

The table reports the risk weights assigned by regulation to the respective cohorts that we observe in our data. Cohorts with the same risk weights are merged in the empirical analysis.

[12] https://www.eba.europa.eu/activities/single-rulebook/regulatory-activities/external-credit-assessment-institutions-ecai/overview-ecais-mapping-under-standardised-approach

B.2 Economic data 2000 to 2024

Table 8: Descriptive statistics of the economic indicators

Variable name	Transformation	Abbrev.	Mean	Std. Dev.
GDP growth rate	log. dif.	g	4.57	1.89
Inflation rate	log. dif.	π	2.59	1.41
Oil price	log. dif.	p	6.98	29.97
10-year real interest rate	rolling mean	i	1.21	0.85
Equity return	rolling mean	e	9.59	19.34

The table reports the economic indicators with the transformation applied to the raw data, their abbreviations, and summary statistics of the transformed series. The first five variables are retrieved from the FRED Database of the Federal Reserve Bank of St. Louis, the series are: GDP, CPIAUCSL, MCOILWTICO, and REAINTRATREARAT10Y. The equity market returns are taken from Kenneth French's data library. In the column Transformation "log. dif" means that the first difference of the natural logarithm of the data is taken with a half year frequency; "rolling mean" means the average over a six-month period is taken. The six-month periods correspond with October 1 to March 31, and April 1 to September 30. The summary statistics are reported in percentages and, for all series except the 10-year rate, annualized. The data ranges from April 2000 to March 2024.

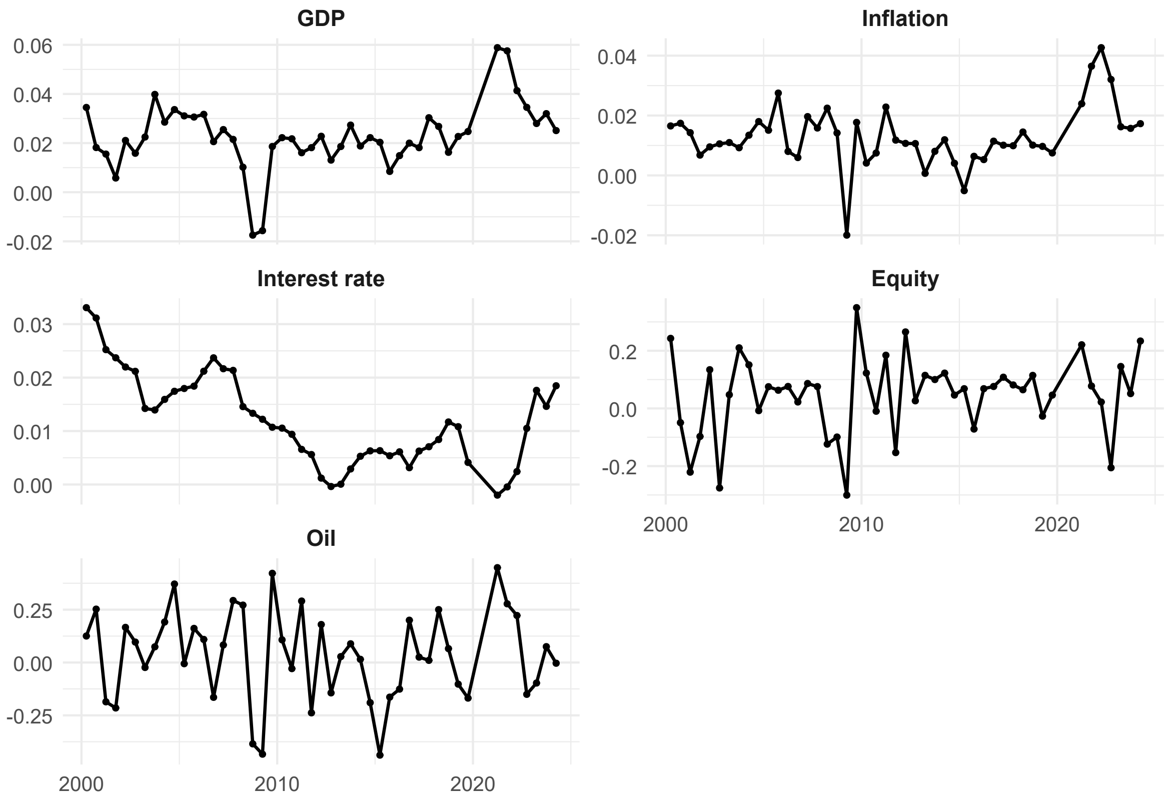

Figure B.1: Economic variables (April 2000 - July 2024)

The figure presents the economic indicators in the US during the in-sample period. The equity returns are computed using the market factor obtained from Kenneth French's data library, all other data are collected from FRED St. Louis FED. *GDP growth*, *Inflation*, and *Oil prices* are measured by log differences, the *10 year Interest rate* is the level of the long-term rates, and *Equity returns* denote average monthly returns.

B.3 Required economic capital in level

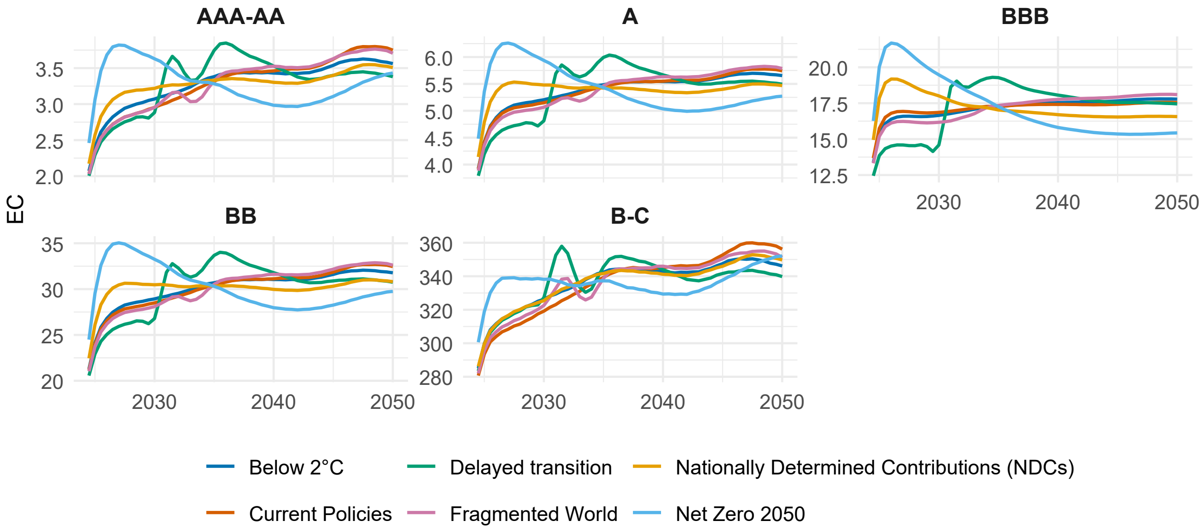

Figure B.2: Economic capital of the different policies based on the REMIND model
The figure presents the effect of the different climate policies on economic capital in basis points up to 2050. Economic capital is calculated as the difference between the 0.999 quantile and the expectation of the loss distribution conditional on the economic indicators and the prediction of the credit cycle in the previous period as given by eq. (13). The quantile follows from eq. (12) and the expectation from eq. (6). The values for μ_{mt} required in these expressions are as constructed and shown in fig. 3, and the values for σ_m are in table 5. The values for the economic indicators are generated using the REMIND model.

B.4 Other Integrated Assessment Models

B.4.1 Results based on the GCAM model

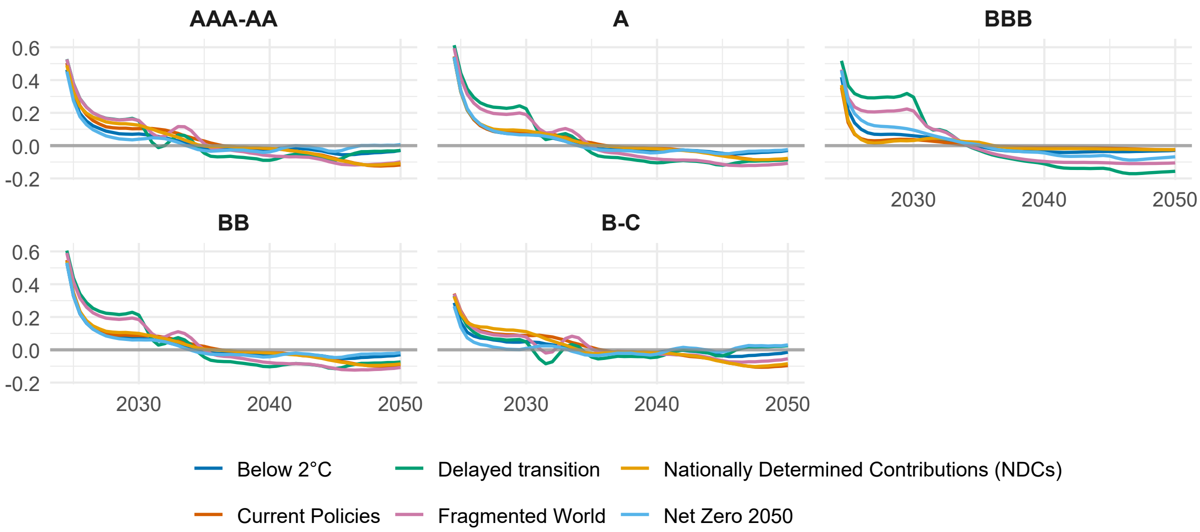

Figure B.3: Predictions for the impact of of transition scenarios on the credit cycle based on the GCAM model

The figure presents the predicted values of the credit cycle for the different cohorts under six different transition scenarios. Predictions are formed based on the model in eq. (5) with parameter estimates in table 5. The values of the economic indicators in the different scenarios are generated by the GCAM model. The predictions take the estimate for the last factor realization Z_{mT} as a staring point. They run from 2024 to 2050.

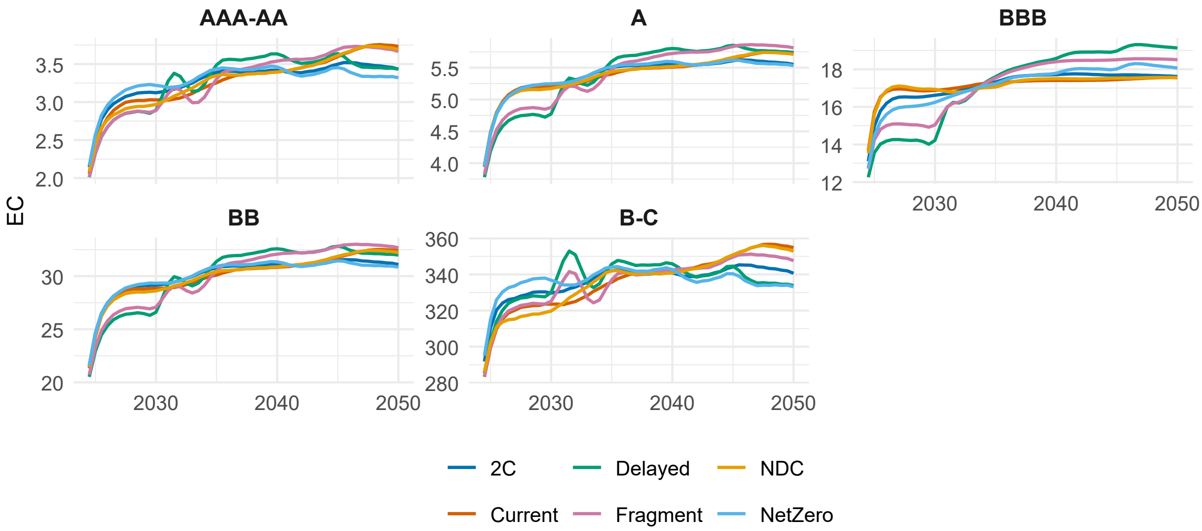

Figure B.4: Economic capital of the different transition scenarios based on the GCAM model
See the note in fig. B.2 for further explanation.

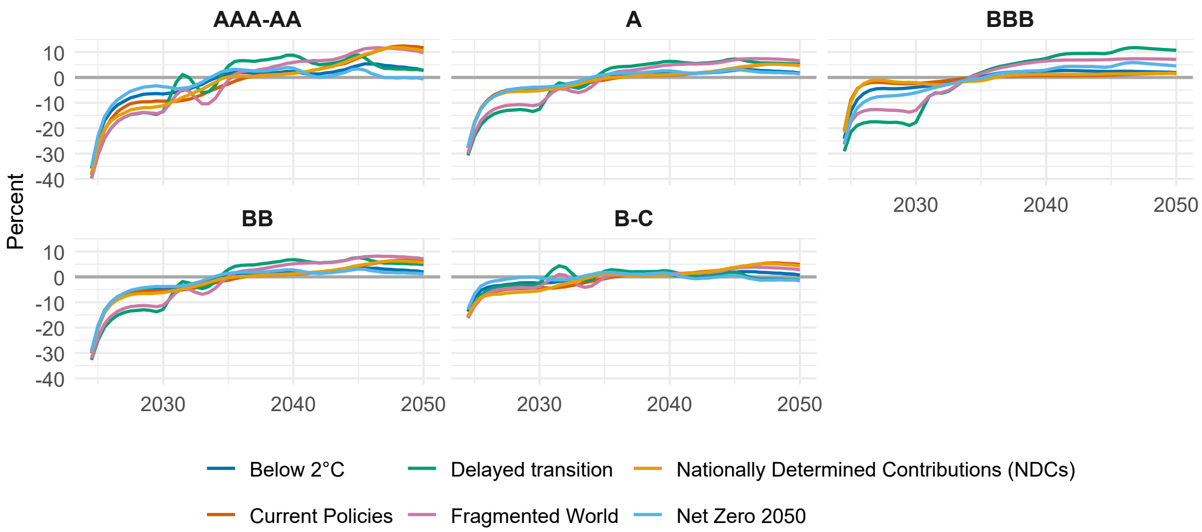

Figure B.5: Changes in EC relative to the neutral state based on the GCAM model
See the note in fig. 4 for further explanation.

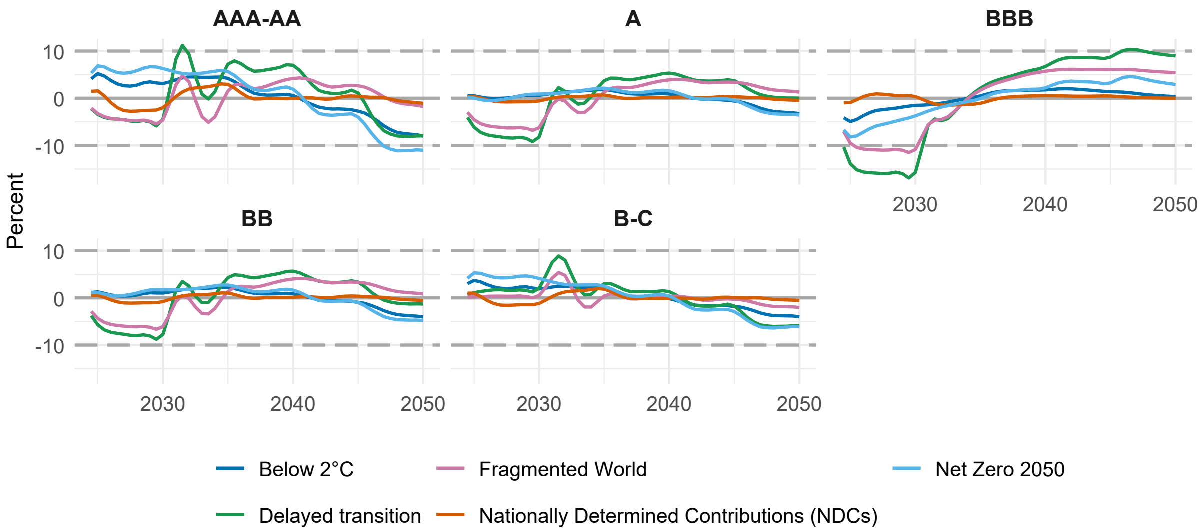

Figure B.6: Changes in EC relative to *Current Policies* based on the GCAM model
See the note in fig. 5 for further explanation.

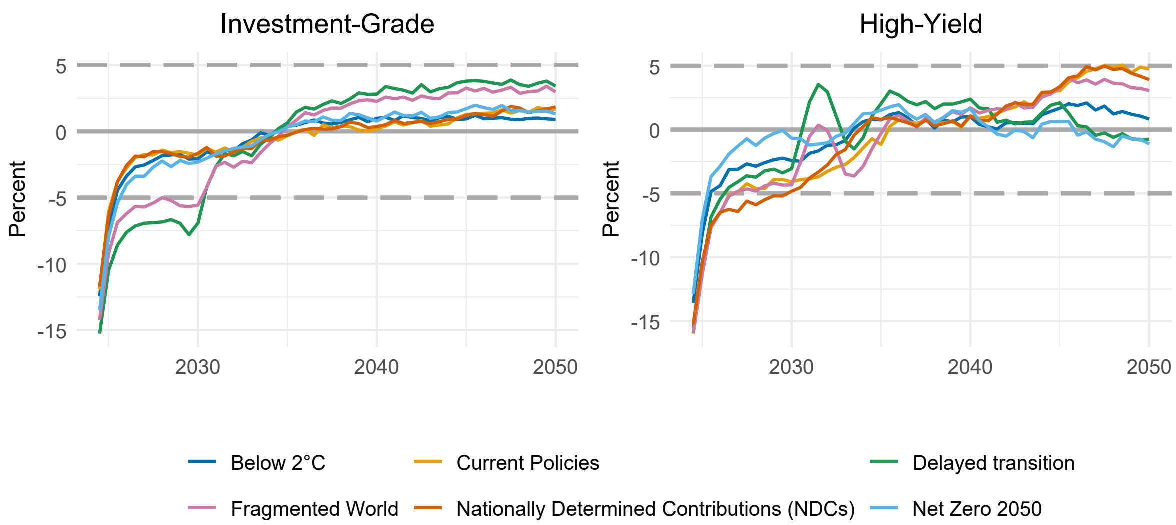

Figure B.7: Changes in EC for heterogeneous bond portfolios relative to the neutral state based on the GCAM model
See the note in fig. 6 for further explanation.

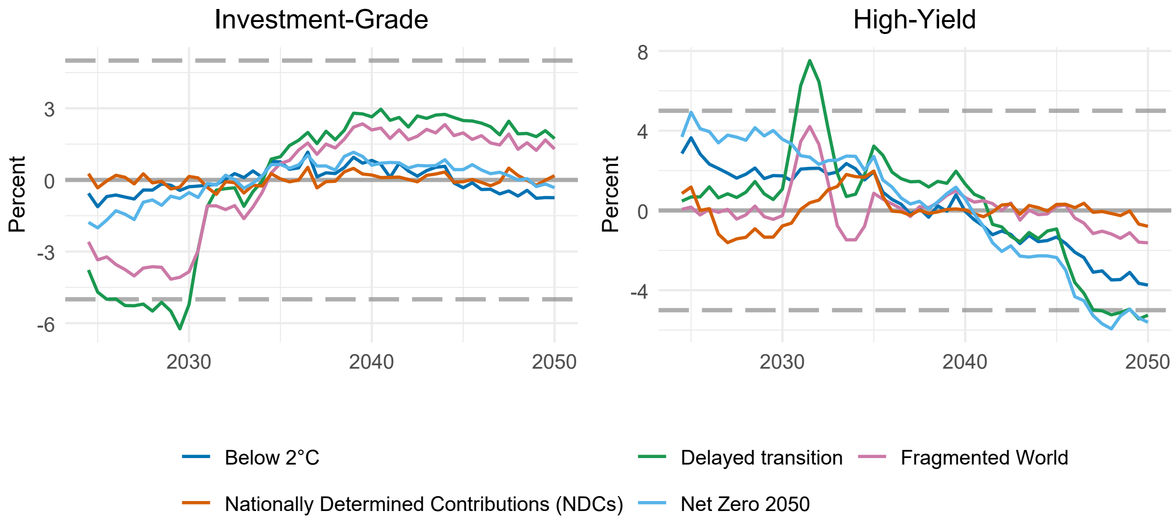

Figure B.8: Changes in EC for heterogeneous bond portfolios relative to *Current Policies* based on the GCAM model
See the note in fig. 7 for further explanation.

B.4.2 Results based on the MESSAGEix model

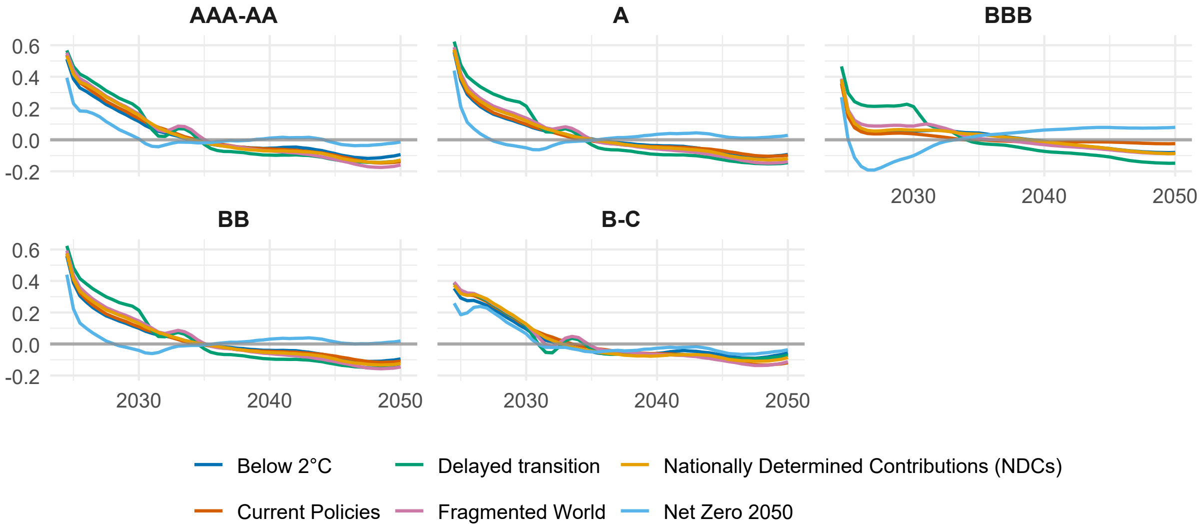

Figure B.9: Predictions for the impact of transition scenarios on the credit cycle using the MESSAGEix

The figure presents the predicted values of the credit cycle for the different cohorts under six different transition scenarios. Predictions are formed based on the model in eq. (5) with parameter estimates in table 5. The values of the economic indicators in the different scenarios are generated by the MESSAGEix model. The predictions take the estimate for the last factor realization Z_{mT} as a staring point. They run from 2024 to 2050.

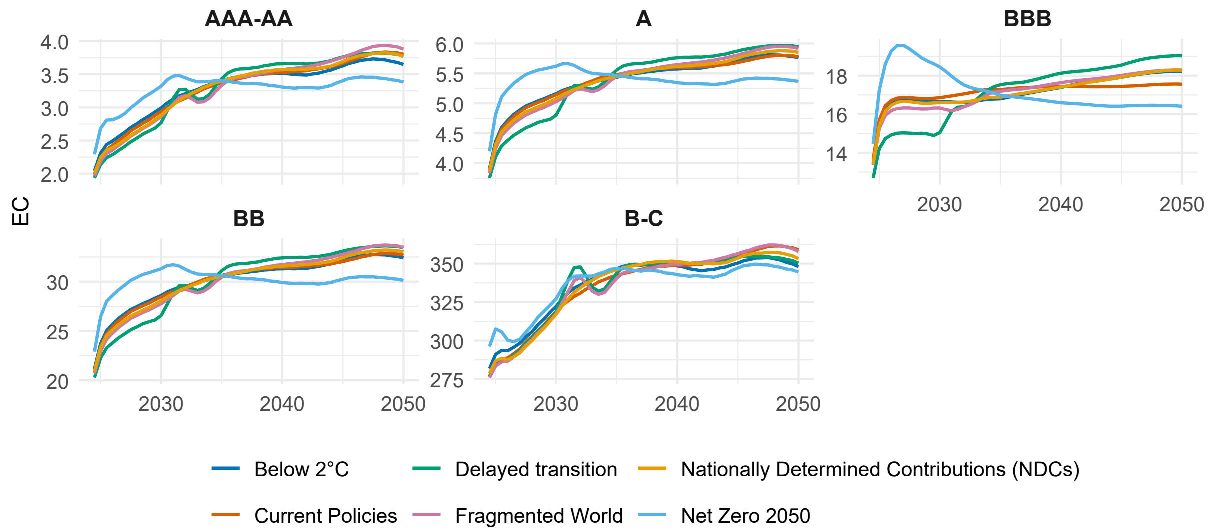

Figure B.10: Economic capital of the different transition scenarios based on the MESSAGEix model

See the note in fig. B.2 for further explanation.

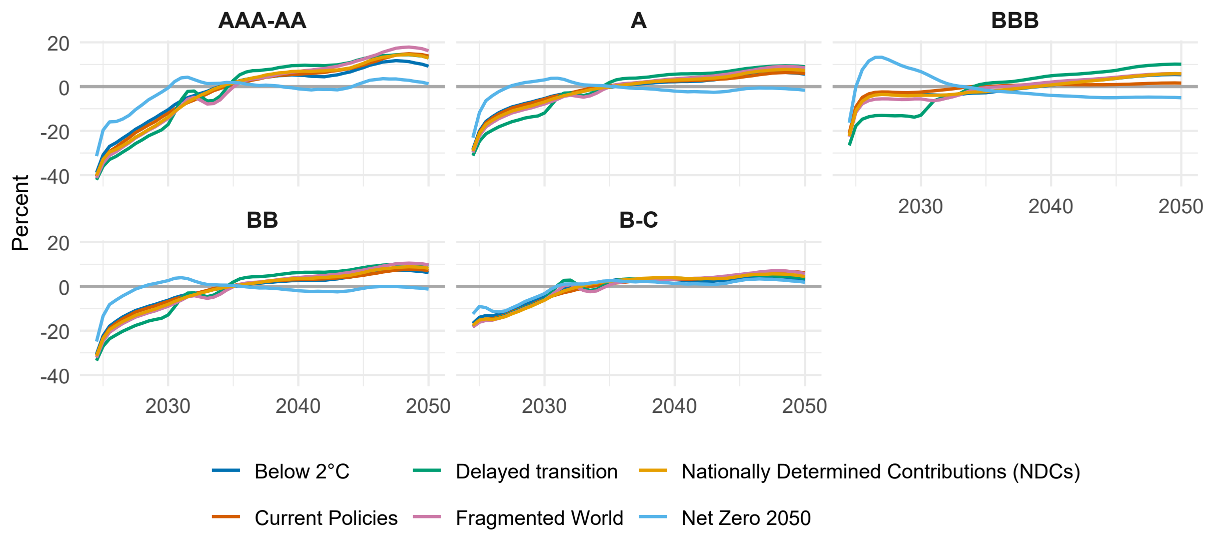

Figure B.11: Changes in EC relative to the neutral state based on the MESSAGEix model

See the note in fig. 4 for further explanation.

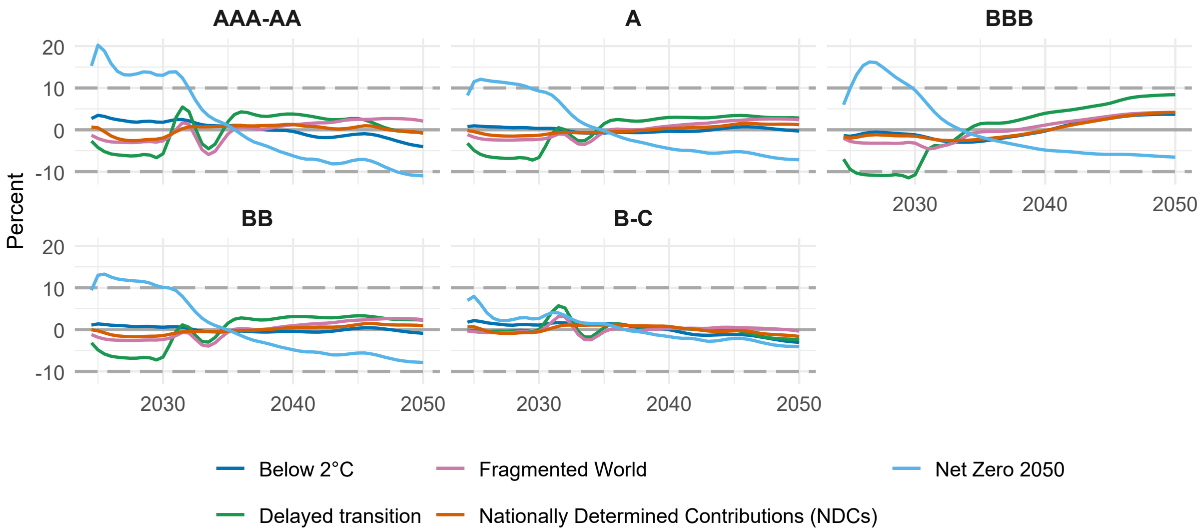

Figure B.12: Changes in EC relative to *Current Policies* based on the MESSAGEix model
See the note in fig. 5 for further explanation.

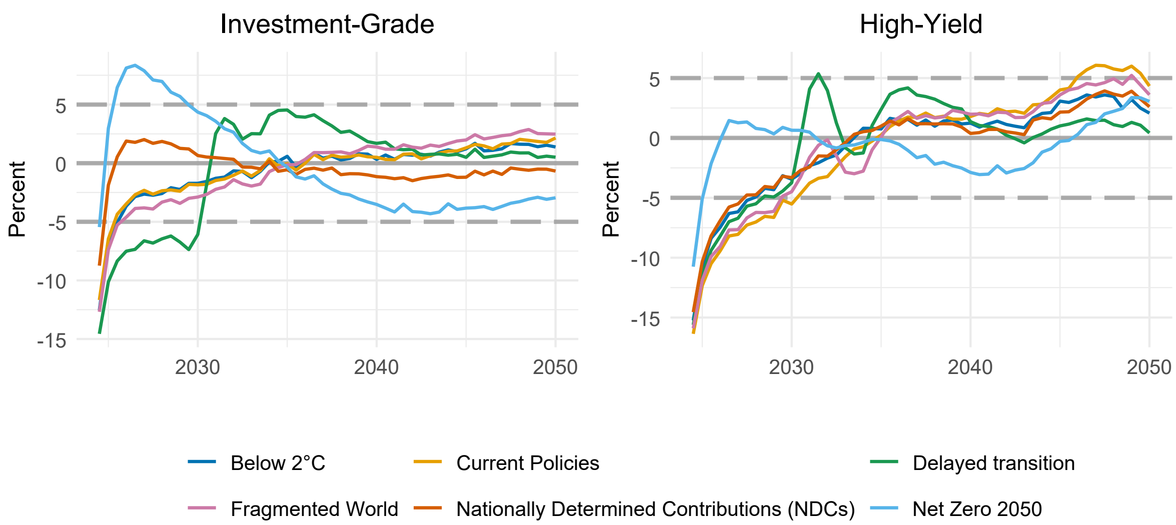

Figure B.13: Changes in EC for heterogeneous bond portfolios relative to the neutral state based on the MESSAGEix model
See the note in fig. 6 for further explanation.

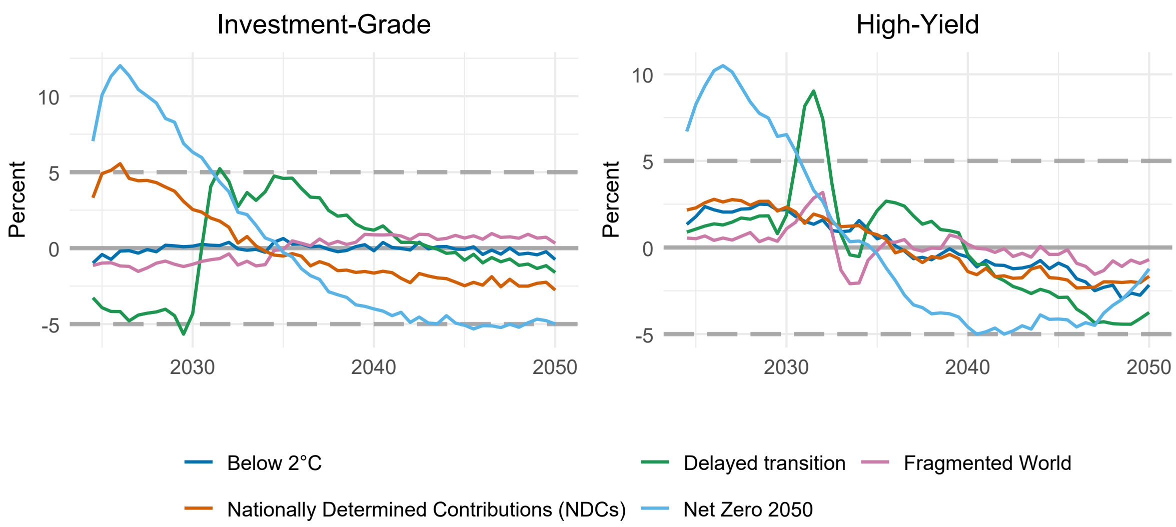

Figure B.14: Changes in EC for heterogeneous bond portfolios relative to *Current Policies* based on the MESSAGEix model

See the note in fig. 7 for further explanation.